

AD-A237 235



2

NAVAL POSTGRADUATE SCHOOL

Monterey, California



DTIC
ELECTE
JUN 20 1991
S B D

THESIS

Circulation of the
California Undercurrent
Near Monterey
in May 1989

by

Alan J. Robson

June 1990

Thesis Advisor:

Curtis A. Collins

Approved for public release; distribution unlimited.

91 6 18 025

91-02436



Unclassified

Security Classification of this page

REPORT DOCUMENTATION PAGE			
1a Report Security Classification Unclassified		1b Restrictive Markings	
2a Security Classification Authority		3 Distribution Availability of Report	
2b Declassification/Downgrading Schedule		Approved for public release; distribution is unlimited.	
4 Performing Organization Report Number(s) NPS-68-90-005		5 Monitoring Organization Report Number(s)	
6a Name of Performing Organization Naval Postgraduate School		7a Name of Monitoring Organization Naval Postgraduate School	
6b Office Symbol <i>(If Applicable)</i> 52		7b Address (city, state, and ZIP code) Monterey, CA 93943-5000	
6c Address (city, state, and ZIP code) Monterey, CA 93943-5000		9 Procurement Instrument Identification Number	
8a Name of Funding/Sponsoring Organization		8b Office Symbol <i>(If Applicable)</i>	
8c Address (city, state, and ZIP code)		10 Source of Funding Numbers	
		Program Element Number	Project No
		Task No	Work Unit Accession No
11 Title (Include Security Classification) CIRCULATION OF THE CALIFORNIA UNDERCURRENT NEAR MONTEREY IN MAY 1989			
12 Personal Author(s) Alan J. Robson			
13a Type of Report Master's Thesis		13b Time Covered From To	14 Date of Report (year, month, day) June 1990
15 Page Count 81			
16 Supplementary Notation The views expressed in this thesis are those of the author and do not reflect the official policy or position of the Department of Defense or the U.S. Government.			
17 Cosati Codes		18 Subject Terms (continue on reverse if necessary and identify by block number)	
Field	Group	Subgroup	

19 Abstract (continue on reverse if necessary and identify by block number)

The path of the California Undercurrent off Monterey in May 1989 was studied using hydrographic data. Water mass analysis compared poleward flowing Undercurrent water with the southward flowing water of the California Current. Isopycnal surfaces and dynamic heights are compared with velocity, water mass properties and bathymetry.

The California Undercurrent was observed to flow poleward off Monterey along the continental slope. Water properties that were most strongly associated with water originating from equatorial regions were found at an average depth of 300 m with the core located between 5 and 25 km off the slope. The width of this water mass varied between approximately 10 and 50 km. These waters are deflected offshore by the shelf topography at Pt. Sur, cross the Monterey Canyon, and turn cyclonically following the shelf past Santa Cruz and Pigeon Pt.

20 Distribution/Availability of Abstract <input checked="" type="checkbox"/> unclassified/unlimited <input type="checkbox"/> same as report <input type="checkbox"/> DTIC users		21 Abstract Security Classification Unclassified	
22a Name of Responsible Individual C. A. Collins		22b Telephone (Include Area code) (408) 646-2673	22c Office Symbol OC/Co

DD FORM 1473, 84 MAR

83 APR edition may be used until exhausted

All other editions are obsolete

security classification of this page

Unclassified

ABSTRACT

The path of the California Undercurrent off Monterey in May 1989 was studied using hydrographic data. Water mass analysis compared poleward flowing Undercurrent water with the southward flowing water of the California Current. Isopycnal surfaces and dynamic heights are compared with velocity, water mass properties and bathymetry.

The California Undercurrent was observed to flow poleward off Monterey along the continental slope. Water properties that were most strongly associated with water originating from equatorial regions were found at an average depth of 300 m with the core located between 5 and 25 km off the slope. The width of this water mass varied between approximately 10 and 50 km. These waters are deflected offshore by the shelf topography at Pt. Sur, cross the Monterey Canyon, and turn cyclonically following the shelf past Santa Cruz and Pigeon Pt.



Accession For	
NTIS GPA&I	<input checked="" type="checkbox"/>
DTIC TAB	<input type="checkbox"/>
Unannounced	<input type="checkbox"/>
Justification	
By _____	
Distribution/	
Availability Codes	
Dist	Avail and/or Special
A-1	

TABLE OF CONTENTS

I. INTRODUCTION.....	1
A. CALIFORNIA CURRENT SYSTEM.....	1
B. BATHYMETRY	2
1. Pt. Sur Platform.....	3
2. Monterey Submarine Canyon System.....	3
3. Santa Cruz Platform	4
C. OBJECTIVES.....	4
II. OBSERVATIONS.....	5
A. CTD	8
B. PEGASUS	8
C. SATELLITE	8
III. RESULTS	9
A. WATER MASS CHARACTERISTICS.....	9
1. T-S properties	9
2. Spiciness anomaly	9
3. Reference profiles.....	11
4. California Undercurrent signature	13
B. PT. SUR SECTION	13
1. Temperature	13
2. Salinity	15
3. Density anomaly	16
4. Spiciness	17
5. Spiciness anomaly	19
6. North/south Pegasus velocity	20
7. East/west Pegasus velocity.....	21
8. Vertical sections of geostrophic velocity.....	22
C. OTHER SECTIONS OF SPICINESS AND DENSITY ANOMALIES...	26

1. Kasler Pt. to Ano Nuevo.....	26
2. Yankee Pt. to Santa Cruz	27
3. Cypress Pt. to Santa Cruz	31
4. Pigeon Pt. (south).....	32
5. Pigeon Pt. (west).....	34
6. Summary	35
D. HORIZONTAL CHARTS OF SPICINESS ANOMALY AND DENSITY ANOMALY DEPTHS	37
1. Layer 1: 25.6-26.0 kg/m ³ γ_{θ}	38
2. Layer 2: 26.0-26.4 kg/m ³ γ_{θ}	40
3. Layer 3: 26.4-26.6 kg/m ³ γ_{θ}	42
4. Layer 4: 26.6-26.9 kg/m ³ γ_{θ}	43
5. Layer 5: 26.9-27.1 kg/m ³ γ_{θ}	46
F. CHARTS OF DYNAMIC HEIGHTS.....	48
1. 0/200.....	49
2. 0/500.....	50
3. 200/500	51
G. HORIZONTAL CHART OF SALINITY AT CORE OF THE CU.....	52
H. AVHRR AND SST IMAGERY	53
IV. DISCUSSION.....	55
A. PATH AND FLOW OF CALIFORNIA UNDERCURRENT.....	55
1. Identification of California Undercurrent.....	55
2. Spiciness anomaly	56
3. Isopycnals	59
4. Dynamic heights	60
5. Effect of bathymetry	61
B. NEAR-SURFACE PATTERNS.....	62

V. CONCLUSIONS AND RECOMMENDATIONS.....66
REFERENCES.....67
APPENDIX A.....68
 CTD DATA CALIBRATION68
INITIAL DISTRIBUTION LIST..... 71

I. INTRODUCTION

A. CALIFORNIA CURRENT SYSTEM

The circulation of the subtropical North Pacific ocean is dominated by a large basin-scale anticyclonic gyre of which the California Current System (CCS) forms the eastern side. The CCS consists of a broad, weak offshore surface flow towards the equator (California Current) plus narrower, stronger nearshore currents at the surface that have been observed flowing either equatorward or poleward (Inshore Countercurrent) or a sub-surface poleward flow (California Undercurrent) found over the continental slope (Chelton 1984).

The California Current (CC) is generally confined to the upper 300 m of the water column, has equatorward velocities less than 25 cm/s, and extends 850 to 900 km from the central California coast as indicated by drogue measurements in previous studies. It is here that water with low temperature and salinity and high dissolved oxygen concentration is transported from high latitudes to the tropics. Within approximately 150 km of the coast the direction of this surface flow reverses toward the pole in the fall and the winter forming the Inshore Countercurrent (IC). This is referred to as the Davidson Current in the area north of Point Conception (Reid and Schwartzlose 1962; Hickey 1979; Chelton 1984).

In the nearshore region below 100 m the flow is predominantly poleward and referred to as the California Undercurrent (CU). Originating in the eastern equatorial Pacific, the water is warm and salty with low dissolved oxygen. The CU shows considerable variability with respect to speed, core depth and offshore position (Hickey 1979). Numerous studies have been conducted using data from

the California Cooperative Oceanic Fisheries Investigations (CalCOFI) beginning in 1949, but most of these data extend to depths of only 500 m with a relatively large horizontal station spacing of 65 km. Between Pt. Conception and Pt. Sur the geostrophic flow in the upper 100 m is generally equatorward from February to September and poleward from October to January. However the flow below 100 m is quite distinct at the two locations. Off Pt. Conception the deeper flow is poleward year round, displaying maxima in June and December, while off Pt. Sur there is maximum poleward flow in December and weak equatorward flow from March to May. Off Pt. Sur, the undercurrent is found approximately 75-100 km from shore (Chelton 1984). Current meter observations indicated poleward flow at all depths off Cape San Martin, approximately 75 km south of Pt. Sur, from 1978 to 1980 with a maximum velocity exceeding 15 cm/s and the core confined to within 30 km of the shore and depths less than 300 m (Wickham et al. 1987). During an 18-month period from February 1984 to July 1985, the Central California Coastal Circulation Study (CCCS) collected current meter measurements, drift buoy trajectories and hydrographic data which all show very strong poleward flow over the continental slope from Pt. Conception to Pt. Sur in June and July (Chelton et al. 1988).

B. BATHYMETRY

Since the Undercurrent is found over the continental shelf and slope, variations of the coastline and bathymetry of the continental margin may have effects on its flow. From Pt. Conception to Monterey, the coastline runs towards the northwest (Figure 1). Unlike the east coast of North America, here the continental shelf is relatively narrow. I will define the upper continental margin as that region between the 200 and 1000 meter contours. At Pt. Conception the width of the

upper margin is about 80 km, then slowly narrows to the northwest with the average width of 15 km south of Pt. Sur. As Monterey Bay approaches, the bathymetry becomes complex. Features include:

1. Pt. Sur Platform

To the west of Pt. Sur the shelf widens from about 12 to 20 km with the distance from shore to the 1000 m contour increasing from 15 to 40 km (Figure 1). Any poleward flow would be forced further from shore by this feature.

2. Monterey Submarine Canyon System

To the north of Pt. Sur the upper margin rapidly decreases to a width of

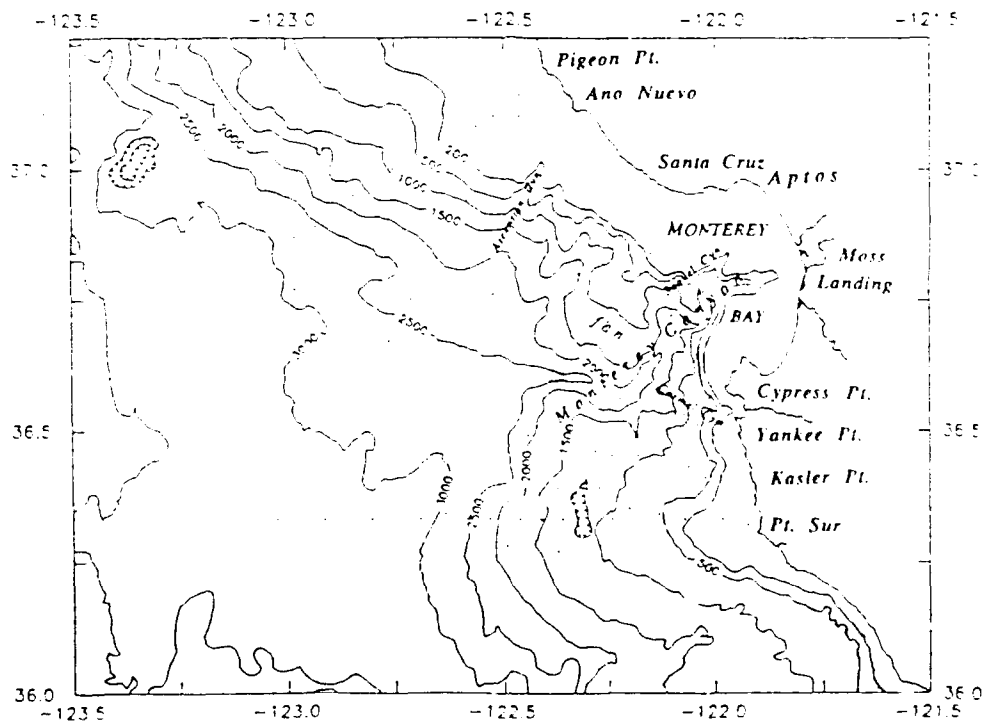


Figure 1. Monterey Bay bathymetry: The bathymetry of the study area is very complex featuring: the deep Monterey Canyon, and the smaller Carmel, Soquel, and Ascension Canyons. Note the fan-like feature south of Santa Cruz. Hatched closed contours indicate decreasing values inside: e.g., seamounts.

less than 4 km off Cypress Pt. with the 1000 m isobath less than 8 km from shore; the continental slope is very steep. The primary bathymetric feature of this region is the Monterey Canyon, which begins at Moss Landing and cuts through the continental slope towards the southwest (Figure 1). At the head of the canyon, a depth of 200 m is reached less than three km from shore at Moss Landing. At a few locations, the wall has a slope as steep as 40 percent with the average more like 10 percent. The canyon has smaller ravine-like features that branch off towards Carmel Bay and Aptos named the Carmel and Soquel Canyons, respectively.

3. Santa Cruz Platform

In the vicinity of Santa Cruz and north past Pigeon Pt, the 200 m isobath is between 15 and 20 km from shore forming a large platform-like feature (Figure 1). Running along the north wall of the Monterey Canyon, the upper margin is still relatively narrow (3 km) until a feature resembling a fan is encountered southwest of Santa Cruz followed by Ascension Canyon south of Ano Nuevo. Here the upper margin broadens to approximately 15 km, then narrows to about 10 km towards the northwest.

C. OBJECTIVES

In May 1989 a large scale survey of the CU was organized by Nan Bray of the Center for Coastal Studies, La Jolla, California. As part of this effort, the Naval Postgraduate School undertook a hydrographic survey in the region between Pt. Sur and Pigeon Pt. to determine how the path of the Undercurrent is affected by the complex local bathymetry. I will utilize these data to this end, applying methodology for defining water masses by their physical characteristics, developed by Lynn and Simpson (1989).

II. OBSERVATIONS

Hydrographic data were collected aboard the *USNS DeSteiguer* between 10 and 26 May 1989. One-hundred ten hydrographic stations were occupied in six sections as depicted in Figure 2 and Table 1. The Pt. Sur section runs due west from Pt. Sur along $36^{\circ} 20' N$, a distance of almost 125 km. It includes stations 1 through 18.

This section was designed to be orthogonal to the local bathymetry. The far end of the section is located over the entrance to the Monterey Canyon in water which is about 3200 m deep. The section parallels the canyon between stations 14 and 18 before turning toward the northwest. Here the canyon depth is almost 400m deeper than the adjacent ocean floor.

The next section runs west-northwest from Kasler Pt. (station 60) to station 51 for a distance of approximately 45 km, then turns north-northwest to station 78 and completes the section towards the north-northeast to Ano Nuevo, ending at station 84. From Kasler Pt. to station 51 this section is perpendicular to the continental margin. It then turns to the north and crosses the canyon. The deepest point of the canyon crossed by this section is 2975 m at station 24. The final part of the section crosses the continental margin perpendicular to the coast.

The third section runs to the northwest from Yankee Pt. (station 41) to station 33 (about 35 km from shore), where it turns to the northeast and ends at station 42 off Santa Cruz. This section also runs orthogonal to the bathymetry out to a depth of 2000 m (station 33), approximately 25 km from shore. Then the section runs orthogonal to the bathymetry, splitting the previously mentioned fan-like feature.

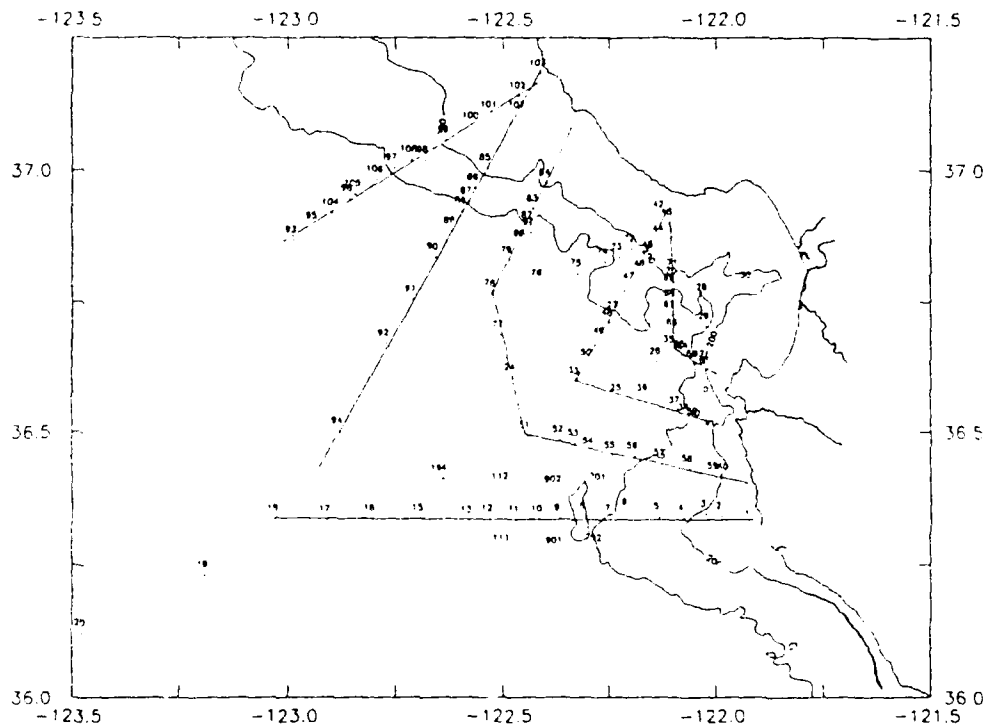


Figure 2. CTD and section locations: One-hundred ten CTD stations were occupied during the survey. Sections were designed to be perpendicular to the continental slope. The upper margin (between 200 and 1000 m) is noted.

The fourth section starts at station 61 off Cypress Pt., continues offshore 15 km to the center of the canyon (station 35) and then turns north, ending also at station 42 off Santa Cruz. This section runs at approximately a 45 degree angle to the bathymetry out to station 35. The remainder of the section into Santa Cruz runs perpendicular to the isobaths.

The fifth section runs from station 107 off Pigeon Pt. towards the south-southwest a distance of 80 km and ends at station 94. This entire section runs perpendicular to the isobaths. The area between the 2000 and 3000 m contours is

broader than anywhere else in the entire region with a very gentle 2 percent grade, though from a depth of 2000 m to the shore the slope is more like 7 percent.

The final section runs from station 103, also off Pigeon Pt., to the southwest towards station 93, a distance of 60 km. This section also runs orthogonal to the isobaths. Unlike the rest of the study area, where the distance between the 100 and 200 m contours is on the order of a couple kilometers, here the distance has increased to almost 13 km. The slope of the continental margin has become very uniform maintaining a grade of 7 percent down to the 3000 m isobath.

TABLE 1. LENGTHS AND STATION NUMBERS OF SECTIONS.

Section	Length (km)	Station numbers
Pt. Sur	125	1-18
Kasler Pt. to Ano Nuevo	125	60-51, 24, 77-84
Yankee Pt. to Santa Cruz	100	41-36, 25, 33, 50-48, 27, 47-42
Cypress Pt. to Santa Cruz	50	61-65, 35, 66-71
Pigeon Pt. (south)	100	85-92, 94
Pigeon Pt. (west)	60	93, 97-108

Several additional stations were located either farther to the west or within the bay and not along any of the sections. Station 0 was located 3 km off Cypress Pt. in Carmel Canyon. Stations 26 and 28-30 were located within Monterey Bay along the center of the canyon. Stations 72-73 and 81 were located southwest of Santa Cruz between stations 44 and 78. Stations 701, 702, 901, 902, 111, 112, and 141 were located either slightly to the north or south of the Pt. Sur section between 40 and 80 km offshore. Stations 19 and 20 were located the farthest offshore, approximately 15 and 30 km, respectively, on a southwest bearing from station 18.

A. CTD

CTD casts were made with a Neil-Brown Mk III CTD at stations ranging from 27 to 3631 m in total depth. Station spacing in the sections varied between 1 and 15 km with 10 km being the average. Bottle samples were collected at selected depths for use in subsequent conductivity calibration. Data calibration techniques are described in Appendix A. Salinity was calculated according to PSS78 and then, along with temperature, averaged over 2 dbar intervals.

Section plots were made of temperature, salinity, spiciness (Lynn and Simpson 1989), spiciness anomaly, density anomaly and geostrophic velocity. Charts of spiciness anomalies over various ranges of density anomaly and dynamic height were also made.

B. PEGASUS

Seven stations were occupied with an acoustically tracked dropsonde called "Pegasus" (Spain, et al. 1981). At each station, two drops were made, about ten hours apart (half the local inertial period). Up and down casts for each of these two drops were averaged to yield horizontal velocity every 25 m. The accuracy and precision are 1 cm/s.

C. SATELLITE

Satellite imagery from the NOAA-9/AVHRR for the period covering 11 to 25 May 1989 was obtained to compare the pattern and evolution of sea surface temperature with hydrographic results.

III. RESULTS

A. WATER MASS CHARACTERISTICS

1. T-S properties

Temperature versus salinity is plotted for all stations at selected depths (Figure 3). Surface salinities ranged between 33.2-33.5 psu; surface temperatures ranged from 10-15°C. The seasonal layer extended from these warm surface values down to approximately 9.5°C and 33.7 psu. The region between 9.5 and 5.5°C was marked by greater salinity variability than that above or below. This is the region of the California Undercurrent where waters of equatorial and subarctic character are found. Although there was a gradation of properties from offshore to onshore, individual casts tended not to be mixed uniformly with depth across this region. Instead intrusions of the different water masses were often present on an individual cast. Below 5°C, temperature dominated the stratification with the lower end of the observed T-S characteristics centered at 34.66 and 1.6°C. These deep waters are characteristic of the Subarctic North Pacific Ocean (Sverdrup, et al. 1940).

2. Spiciness anomaly

To trace the waters of the CU, I calculated an anomaly of spiciness using a procedure similar to Lynn and Simpson (1989). Spiciness, calculated according to the method of Flament (1989), is a direct measure of the differences between temperature-salinity properties in a direction along constant density anomaly lines. At a given density anomaly, water that is warmer and saltier has a higher spiciness than water that is cooler and fresher. To calculate a spiciness anomaly,

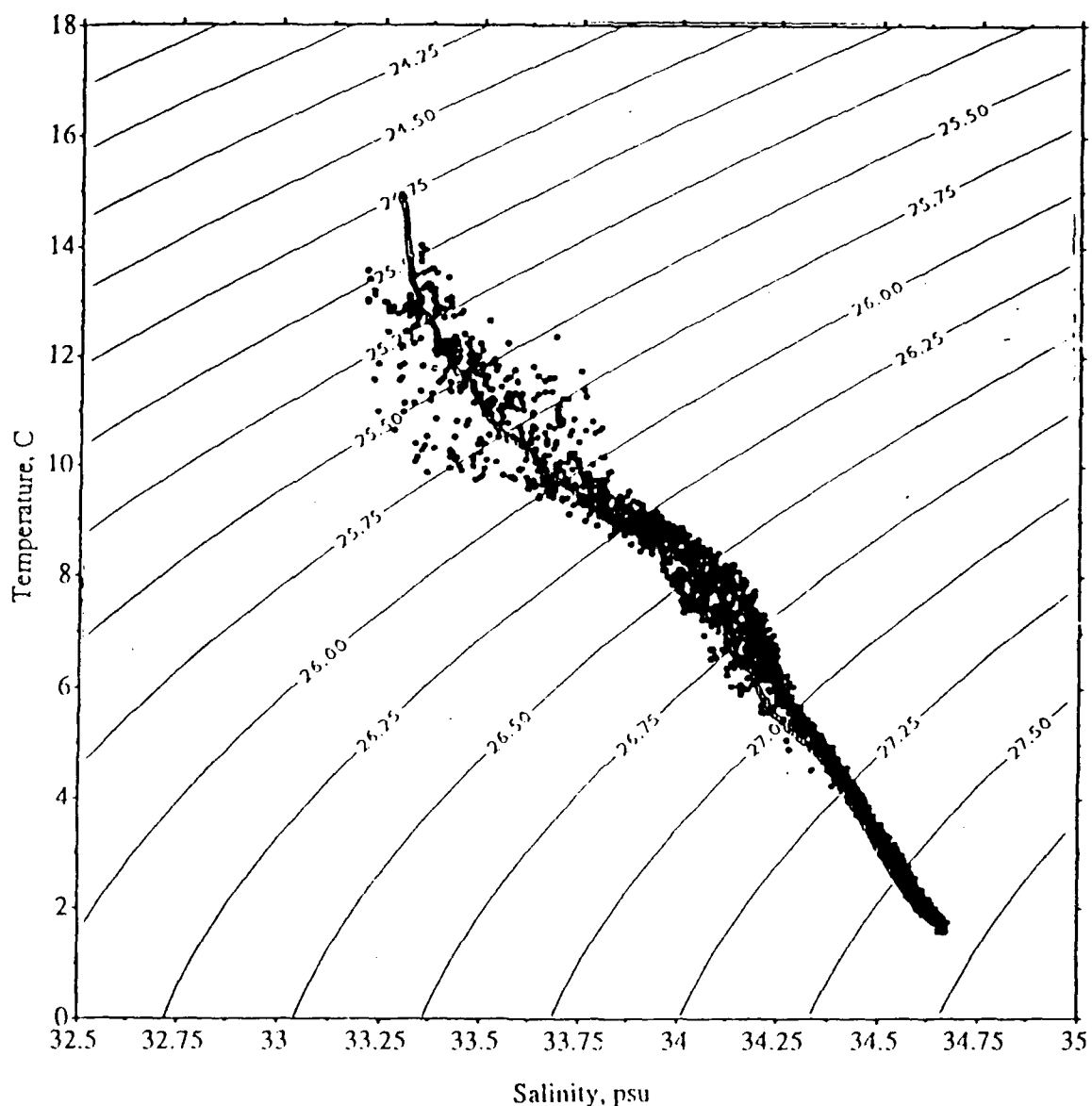


Figure 3. T-S diagram for all stations: Temperature versus salinity plotted for all CTD stations at selected depths. Great variability of temperature and salinity was observed in the upper layers. Between 9.5 and 5.5°C, variations in salinity were observed indicating the mixing of saltier equatorial CU water with offshore CC water. Deep water ($\sigma_t > 27.0$) displayed characteristics of North Pacific Sub-Arctic water. The reference T-S curve denotes the average of the eight stations used to calculate the spiciness anomaly.

spiciness from eight CTD profiles (stations 14-20 and 94) were averaged together over constant density anomaly levels of 0.01 kg/m^3 . The eight stations were chosen as they were the farthest offshore and displayed characteristics of Sub-Arctic water in this region. These stations did display some signs of interleavings and mixing, and were not particularly smooth. Spiciness anomalies from the mean spiciness curve of these eight stations were then computed for each station.

3. Reference profiles

Vertical profiles for the averaged reference stations are illustrated in Figure 4. Surface properties were 14.9°C , 33.29 psu , 24.68 kg/m^3 and 0.7585 spiciness. The strongest vertical gradients were found in the upper 50 m and correspond to changes of 4.5°C , 0.3 psu , 1.1 kg/m^3 , and 0.6561 spiciness. Below this layer, the temperature gradient was 0.02°C/m , the salinity gradient was 0.004 psu/m , and the density gradient was 0.0066 kg/m^4 in the lower part of the seasonal layer which extended to approximately 150 m. Spiciness reached a relative minimum of 0.0398 at 91 m, then increased slowly to a relative maximum of 0.0884 at 165 m before starting to decrease again. Here the warmer and fresher waters which are found offshore dominated the profile. Gradients associated with the "main" thermocline from 200 m to 2000 m were 0.003°C/m , 0.0003 psu/m , and 0.0005 kg/m^4 . From 2000 m to the bottom at 3300 m, the gradients were 0.0005°C/m , 0.00015 psu/m , and 0.00016 kg/m^4 . Below 1000 m spiciness decreased uniformly with a gradient of $0.000029 / \text{m}$.

The reference T-S curve for the eight averaged stations (described below) is shown superimposed on the T-S data for all the stations in Figure 3. Between 9.5 and 14°C and 33.2 and 33.8 psu , representing the surface waters, the reference curve was centered fairly well, though the majority of the data appeared to the

right of the reference profile (spicier than the reference). In the seasonal layer (down to approximately 9.5°C and 33.7 psu) almost all of the data were to the right of the reference T-S curve. At 8°C the reference curve moved closer to the middle of the data, though more points were still located to the right of the reference curve.

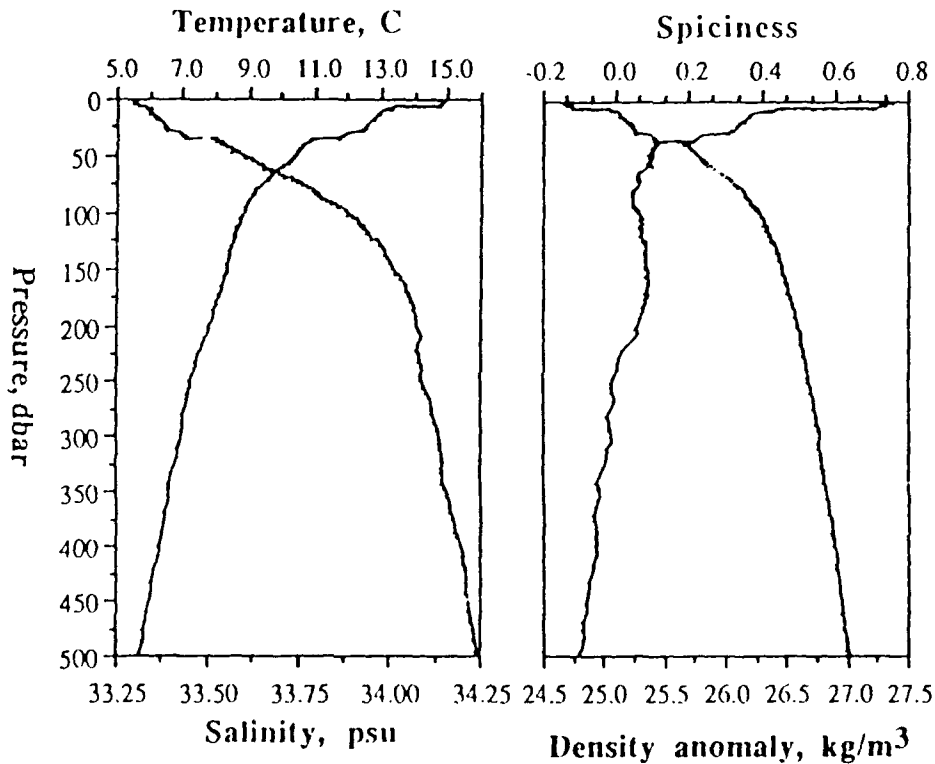


Figure 4. Reference profiles: Vertical profiles of temperature, salinity, density anomaly and spiciness anomaly for upper 500 m of averaged reference stations.

Between 8 and 7°C, the reference curve became isohaline. The isohaline layer started at a depth of approximately 180 m with a temperature of 7.98°C, salinity of 34.070 psu, spiciness of 0.0730, and density anomaly of 26.58 kg/m³. The bottom of the layer was at 230 m with a temperature of 7.39°C, salinity of 34.077 psu, spiciness of -0.0006, and density anomaly of 26.64 kg/m³.

Interestingly, it is at the lower boundary of this layer that spiciness became zero. The spiciness gradient in this isohaline layer was $0.0014/\text{m}$, which was greater than anywhere in the profile except at the surface .

Below the isohaline layer, the reference T-S curve was once again at the left margin of the data with the same slope and shape. It ended at the same point as the main T-S curve (1.6°C and 34.66 psu).

4. California Undercurrent signature

Following the method of Lynn and Simpson (1989), I will utilize spiciness and density anomalies to identify the water masses in the study area. In this context, subsurface water having an anomaly of $+0.04$ from the reference spiciness curve and a density anomaly value between 26.6 - 26.9 kg/m^3 is correlated with the warmer, saltier water carried poleward from the tropics by the California Undercurrent. The dynamic signature of a subsurface poleward flow are isopycnals which slope downward toward the coast. The strength of the baroclinic poleward flow is determined by the slope of the isopycnals.

B. PT. SUR SECTION

I begin by describing the water properties and velocity for the Pt. Sur section. For the duration of the study, winds were predominantly northwesterly, except for one relaxation event, resulting in upwelling.

1. Temperature

As seen in Figure 5a, surface waters were warmer than 11°C , except at stations 1 and 3 where temperatures were 10.77 and 10.98°C , respectively. Sharp horizontal temperature gradients (fronts) were not present. The seasonal thermocline was marked by waters warmer than 8.5°C , which occur above about 150 m. There were undulations of the seasonal thermocline of about 25 m, but the

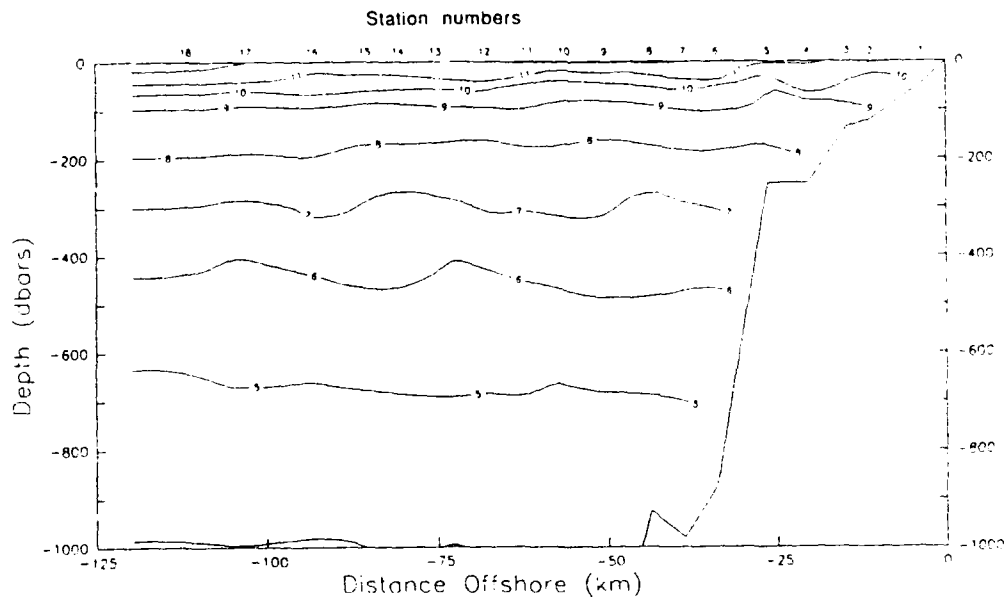


Figure 5a: Pt. Sur temperature: The vertical section of temperature ($^{\circ}\text{C}$) for the Pt. Sur transect showed upwelling in the upper 100 m near the coast and downward sloping isotherms near the coast at depths greater than 200 m caused by the presence of warmer CU water.

major characteristics were the intensification associated with surface warming offshore at stations 17 and 18, and the upwelling of isotherms inshore of station 6. The latter was not represented by a steady shoaling of isotherms toward the coast; instead isotherms shoal at stations 5 and 2. Next to the coast, isotherms associated with seasonal thermocline deepened.

Waters associated with the main thermocline (4 to 8°C) occupied the remainder of the water column to about 1000 m. The 7 and 8°C isotherms were nearly level at about 300 and 200 m, respectively. The 4 , 5 , and 6°C isotherms deepened gradually toward the coast, indicating the warmer temperatures associated with water derived from the Equatorial Pacific. Imposed on these trends of isotherm depth were two or three undulations; these had maximum

amplitude at 6 and 7°C, about 50 m, and were not in phase at all depths. At the coast, the isotherms associated with the main thermocline also sloped down toward the coast.

2. Salinity

Salinity for the Pt. Sur section is shown in Figure 5b. Surface waters were fresher than 33.6 psu except at stations 2 and 3, where the surface salinities were 33.602 and 33.627 psu, respectively. The seasonal halocline was marked by waters fresher than 34 psu. These isohalines have the same pattern as the isotherms associated with the seasonal thermocline; they are nearly level with 25 m undulations. The isohalines upwell inshore of station 6 but are depressed at the coast. At stations 17 and 18, the seasonal halocline deepens and becomes more intense. In contrast to the upper 200 m, the isohalines below 200 m do not parallel

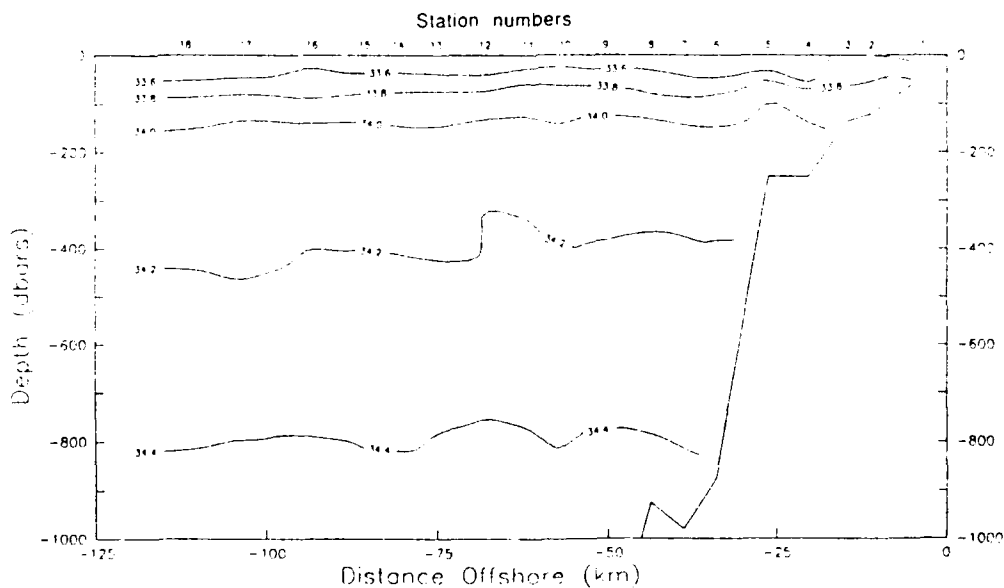


Figure 5b. Pt. Sur salinity: The vertical section of salinity (psu) for the Pt. Sur transect indicated upwelling at the coast in the upper 100 m.

isotherms, indeed, they tend to behave in an opposite manner. Both 34.2 and 34.4 psu isohalines slope up toward the coast and the pattern of undulations is out of phase. At the coast, the 34.4 psu isohaline downwells while the 34.2 psu isohaline is nearly level. Clearly, waters below 200 m are saltier at a given depth inshore than offshore. Near stations 11 and 12, approximately 65 km offshore, the 34.2 psu isohaline makes an almost 100 m excursion toward the surface. Recall from the earlier discussion of reference profiles that offshore waters contained an isopycnal layer at about 34.1 psu.

3. Density anomaly

Density is represented by a density anomaly, which is calculated using a potential temperature (θ) referenced to 0 dbar. Using the notation of the 1980 equation of state (UNESCO,1987):

$$\gamma_{\theta} = \rho(S, \theta, p, 0) - 1000 \text{ kg/m}^3$$

This has the advantage of giving a truer representation of isopycnal surfaces. I will refer to this quantity as "density anomaly".

Density anomaly for the Pt. Sur section is shown in Figure 5c. Surface waters were lighter than 25.6 kg/m^3 over the entire length of the section, except inshore of station 5 where values ranged from 25.62 kg/m^3 at station 1 to 25.71 kg/m^3 at station 3. At stations 17 and 18 density was less than 25.4 kg/m^3 , as was the case between stations 10 and 7. In the upper hundred meters the vertical gradient of density was considerably greater offshore than nearshore. This pattern of upwelling of shallow isopycnals toward the coast suggests an equatorial flow offshore in the upper 200 m. The 26.4 kg/m^3 isopycnal shoaled 25 m at station 5 then sloped down toward the coast.

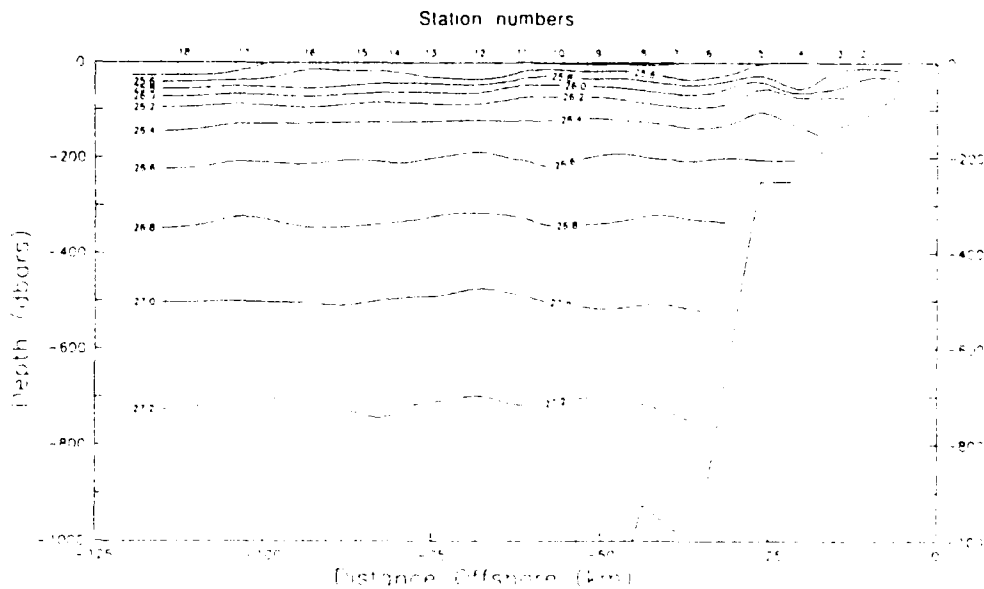


Figure 5c. Pt. Sur density anomaly: The vertical section of density anomaly (kg/m^3) for the Pt. Sur transect showed upward sloping isopycnals in upper layers indicating upwelling, and downward sloping isopycnals below 200 m indicating poleward flow.

Below 200 m, the 26.6 and 26.8 kg/m^3 isopycnals were basically level, with a few slight undulations that were in phase with each other. The 27.0 and 27.2 kg/m^3 isopycnals followed the same pattern, however they sloped down toward the coast inshore of station 12.

4. Spiciness

The spiciness section (Figure 5d) shows a great deal of structure. Largest values of spiciness (exceeding 0.12) were found at the surface with values greater than 0.28 at stations 11 (0.30) and 12 (0.36) indicating the warmest and saltiest water at this location. The 0.12 contour is basically level seaward of station 11, while shoreward it shoals from 100m to the surface at station 5, then returns to a depth of 50 m to the coast. At 100 m, the lowest values of spiciness are

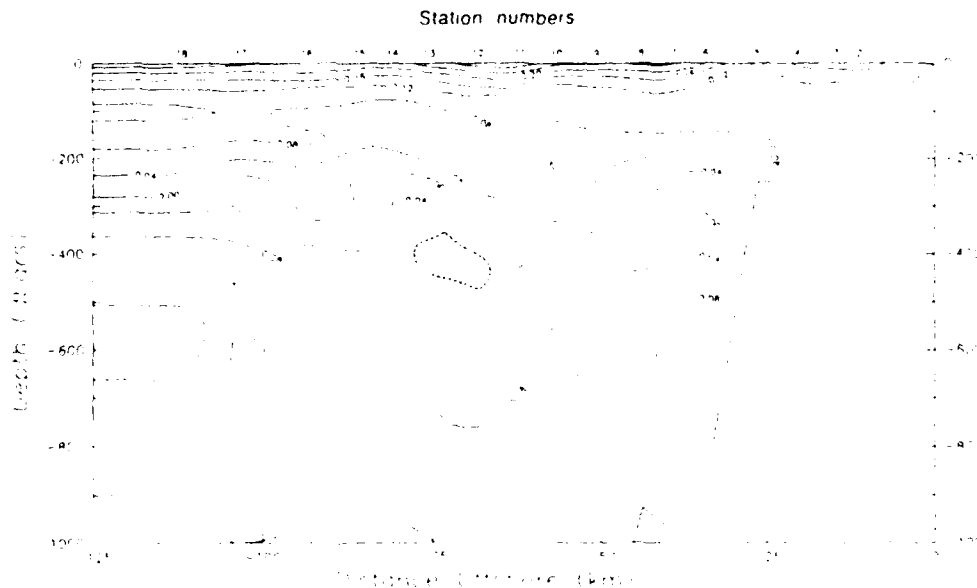


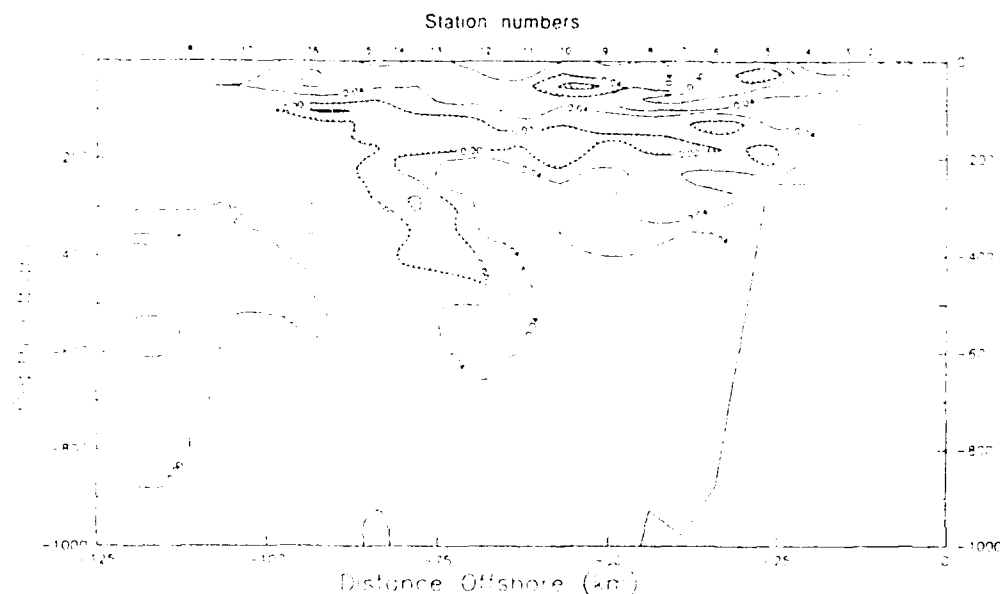
Figure 5d. Pt. Sur spiciness: Spiciness for the Pt. Sur section were high in the surface layers, indicating warmer, saltier water. Near the coast the spiciness was higher than that offshore indicating the presence of the warmer, saltier CU of equatorial origin.

found at station 14. Below this level, lowest values of spiciness were found offshore. At stations 17 and 18 the distance between the +0.08 and -0.08 contours was approximately 200 m with the center, indicated by the zero contour, at about 300 m depth. Inshore the gradient between these two contours relaxed considerably with the distance widening to over 600 m at station 13, then narrowing to 300 m where this layer was at the coast at station 5. The depth of the zero contour undulated ± 50 m with the average depth remaining 300m, and gradually deepened toward the coast. Between stations 12 and 13 there was an area of less than -0.08 spiciness at 400 m depth (hatched in Figure 5d). Inshore of this feature, the -0.04 through 0.08 contours sloped down to the coast. At station 10 there was a shoaling of 100 m in the -0.08 contour that was reflected, though not as

strongly, in the spiciness contours above. To the west of this feature the -0.08 contour was at a depth of 750 m (station 10), and to the east it was at 700 m (station 9), thence sloped up to 500 m at the coast. At the coast, spiciness was less than it was offshore at all depths.

5. Spiciness anomaly

Spiciness anomaly, calculated by subtracting the spiciness of the reference profile (Figure 3) from the observed spiciness, is depicted for the Pt. Sur section in Figure 5e. A region of negative anomalies at 200 m separated surface and deep water masses, both of which were positive. At stations 13 and 14 this negative anomaly extended to 400 m, dividing inshore waters from offshore,



the former had higher spiciness than the latter. This negative anomaly defines the cooler, fresher Sub-Arctic water mass. Inshore, the largest sub-surface maxima of spiciness anomaly was found centered approximately 60 km offshore at a depth of 300 m. The anomaly was greater than 0.04 and extended from 200 to 600 m with a maximum distance offshore of 75 km, clearly indicating the presence of warmer, saltier tropical water. Below the 0.04 anomaly area no further anomalies were noted.

6. North/south Pegasus velocity

The vertical section of north ($V > 0$)/south velocity (Figures 6a and 6b) at Pt. Sur showed primarily poleward flow to a depth of about 2400 m and to a distance of approximately 75 to 100 km offshore. Speeds of 21 cm/s or greater were found at the innermost Pegasus station, P1. While the vertical plot of

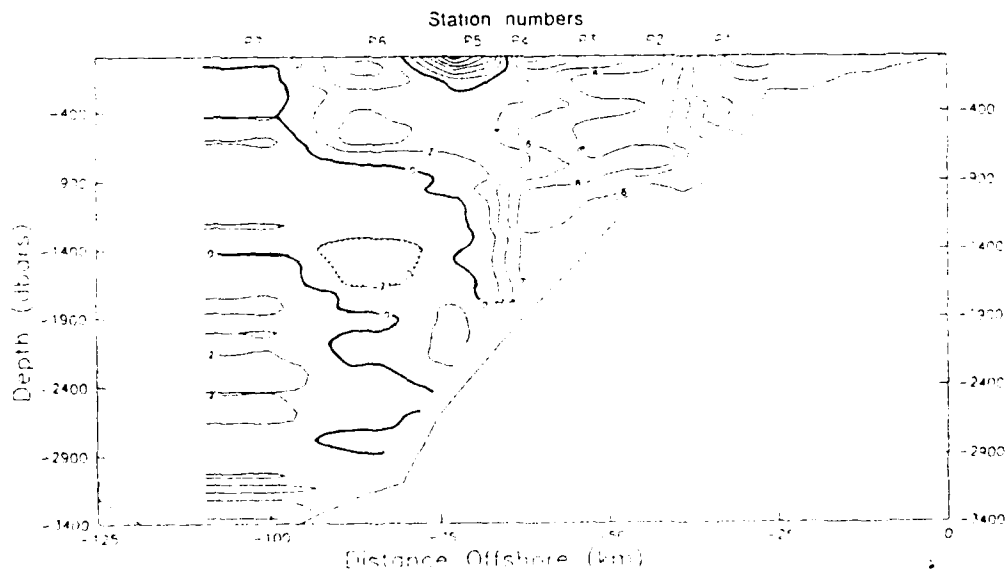


Figure 6a. Pt. Sur Pegasus north/south velocity: Vertical section of Pegasus north/south velocity for Pt. Sur section from surface to 3400 m. A level of no motion at 2400 m was observed.

spiciness anomaly at Pt. Sur (Figure 5e) showed a maximum area (which I interpret as the core of the CU) centered at approximately 60 km from shore, the Pegasus plot showed the velocity increasing from 4 cm/s at 60 km offshore to a maximum of 21 cm/s at 30 km (P1). In the vicinity of P1 the isotachs were vertical. However, at 70 km (P5) there was an equatorward jet of -10.0 cm/s at the surface. The greatest shear was shown between P4 and P5 (60 km offshore) between depths of approximately 800 to 2500 m. The horizontal shear across this 15 km zone was about 6 cm/s. At P2 a vertical shear of approximately 10 cm/s between a depth of 1000 m and the bottom at 1500 m. However a lack of data within the inner 25 km of the section made a determination of the maximum meridional speeds impossible. Beyond station P7, 100 km offshore, the observed velocity became zero. This was also true below depths of 2400 m. Thus a level of no motion for future geostrophic computations of 2400 m is recommended.

7. East/west Pegasus velocity

East ($U > 0$)/west velocity measurements along the Pt. Sur section are shown in the plot of Pegasus U velocity (Figures 7a and 7b). In the upper 1000 m flow was generally to the west, or offshore. At the two closest inshore stations, P1 and P2, the onshore flow reached speeds of 10 cm/s extending to a depth of 200 m, and was generally from 2 to 4 cm/s onshore to a depth of 1500 m. Like the alongshelf velocity, the cross-shelf velocity showed a flow reversal at P5 with onshore flow of 12 cm/s at the surface. Between stations P6 and P7 offshore flow was greater than 10 cm/s at a depth of 100 m and 6 cm/s at 800 m.

8. Vertical sections of geostrophic velocity

Geostrophic velocity was calculated and plotted referenced to a 2000 m level of no motion for the Pt. Sur section (Figure 8a). The geostrophic flow was characterized by alternating bands of poleward and equatorward flow reaching

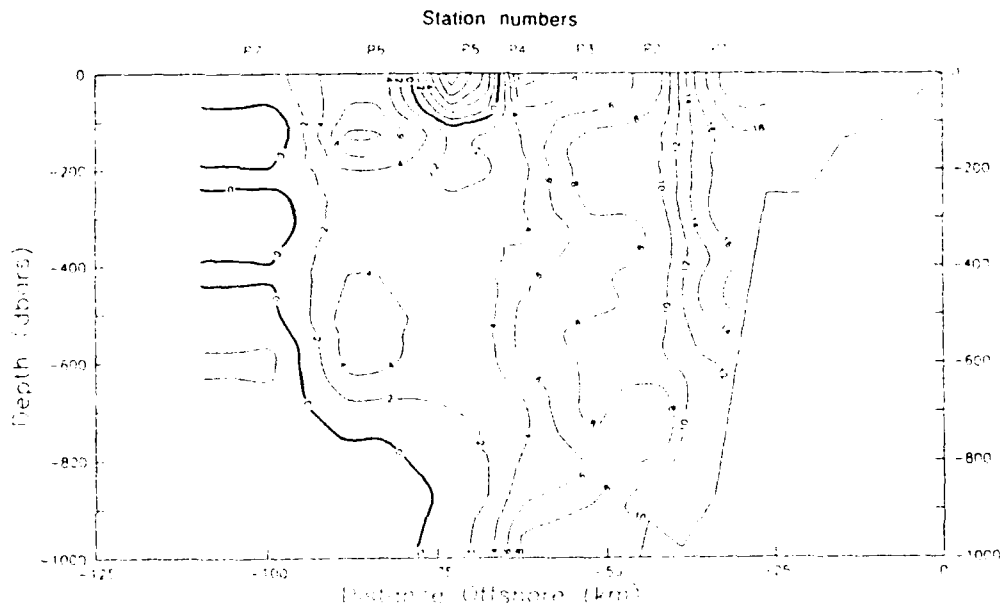


Figure 6b. Pt. Sur Pegasus north/south velocity: Vertical section of Pegasus north/south velocity for Pt. Sur section from surface to 1000 m. Poleward flow ($V > 0$) was measured from the coast to almost 100 km offshore.

maximums of up to 80 cm/s equatorward and 44 cm/s poleward (Figure 8b) with poleward flow indicated between stations 4 and 5, 6 and 8, 10 and 12, and 14 and 17. This does not appear to correlate at all with the Pegasus velocity field.

To reduce station-to-station variability, I smoothed the geostrophic velocity field in the horizontal over a length scale on the order of the Rossby radius of deformation, or approximately 20 km. This section (Figure 9) more closely resembled the Pegasus velocity (Figure 6a), but still showed numerous flow

reversals. With the exception of station 9, the geostrophic flow was poleward from the shore to station 12 (65 km) with a maximum velocity of 25 cm/s at station 7. This compared favorably with the Pegasus results in the region. The geostrophic velocity then reversed again strongly towards the equator between stations 12 and 15 with a maximum velocity of -35 cm/s shown in the vicinity of station 13. An equatorward flow was observed in the Pegasus velocity in the same position. However, the Pegasus jet was much weaker (-10 cm/s versus -35 cm/s) and was only seen in the upper 200 m. From station 15 to station 17 the geostrophic velocity was poleward again, showing a maximum of 15 cm/s between station 15 and 16. This poleward flow was similar to Pegasus, but almost double the velocity. The geostrophic flow then became weakly equatorward again further offshore, where the Pegasus velocity was near zero.

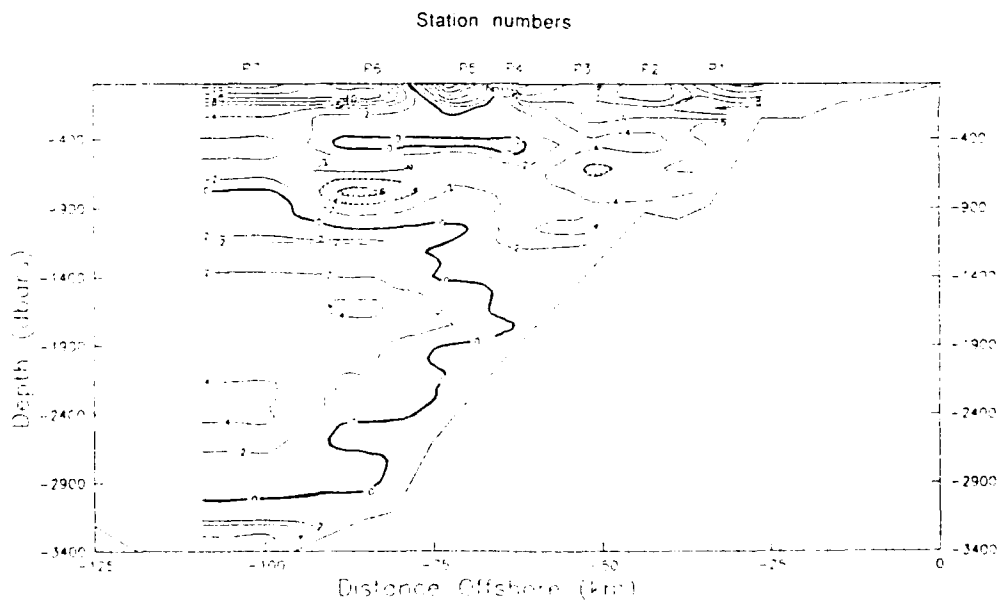


Figure 7a. Pt. Sur Pegasus east/west velocity: Vertical section of Pegasus east/west velocity for Pt. Sur section from surface to 3400 m. Offshore, or westerly flow ($U < 0$) was observed.

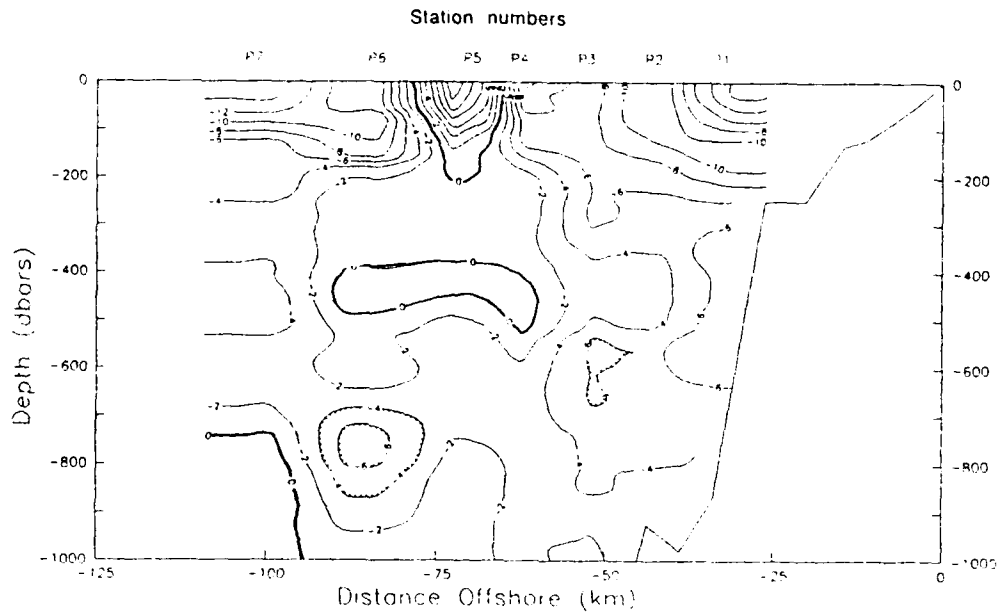


Figure 7b. Pt. Sur Pegasus east/west velocity: Vertical section of Pegasus east/west velocity for the Pt. Sur section from surface to 1000 m.

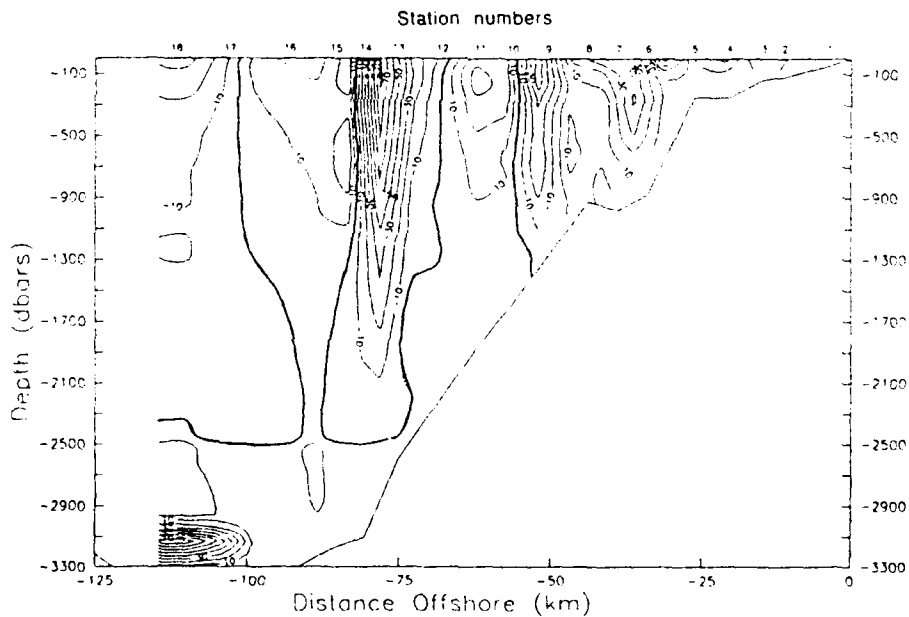


Figure 8a. Pt. Sur geostrophic velocity: Vertical sections of geostrophic velocity for Pt. Sur section from surface to 3300 m., using a level of no motion of 2400 m. Numerous flow reversals were indicated by the banded structure.

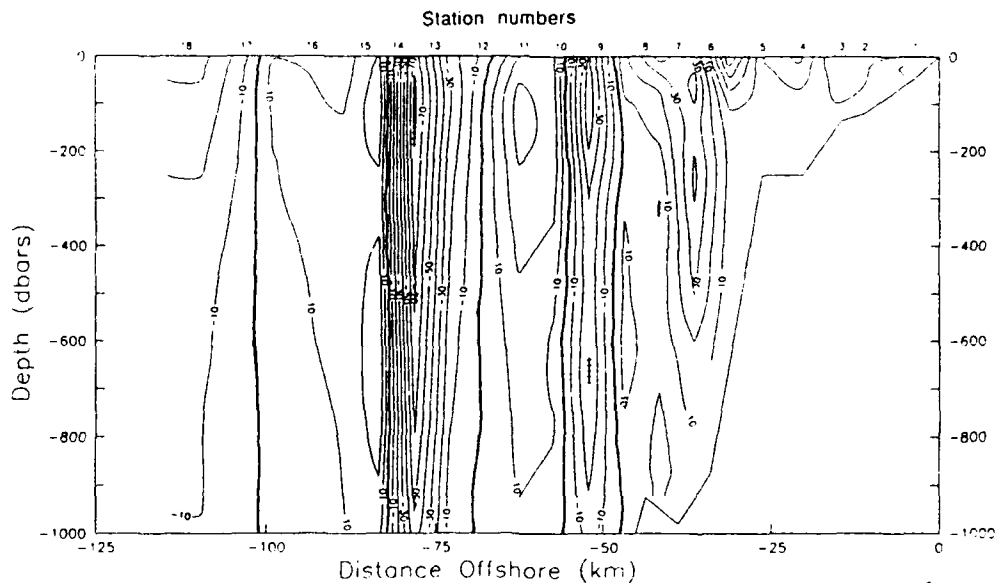


Figure 8b. Pt. Sur geostrophic velocity: Vertical section of geostrophic velocity for Pt. Sur section from surface to 1000 m.

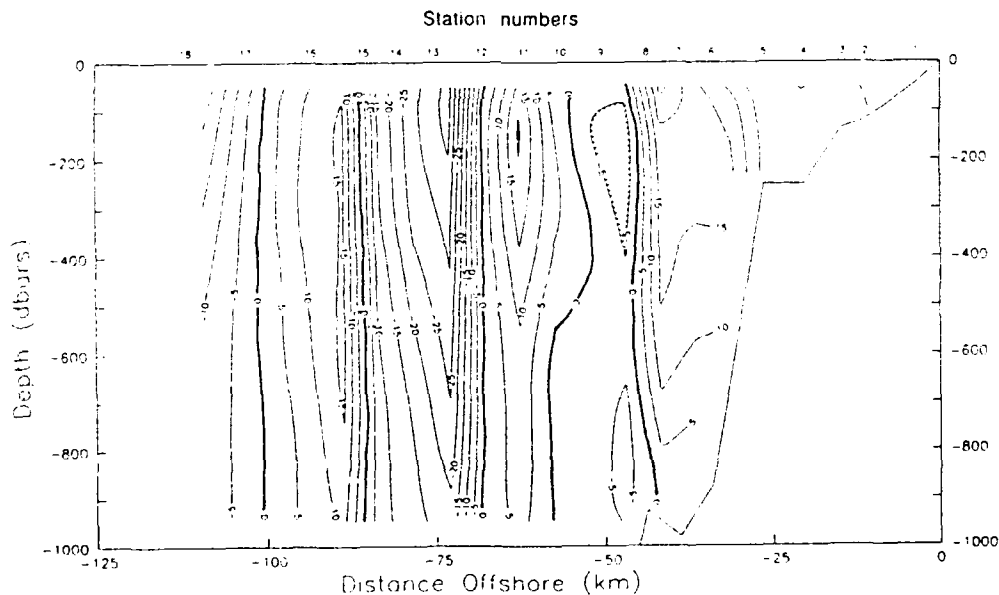


Figure 9. Pt. Sur smoothed geostrophic velocity: Geostrophic velocities for the Pt. Sur section were smoothed to the Rossby radius of deformation (20 km). This resulted in lower overall velocities, but the flow reversals were still present.

C. OTHER SECTIONS OF SPICINESS AND DENSITY ANOMALIES

All sections indicated large positive and negative spiciness anomalies in the upper 50 m, particularly within Monterey Bay. This is indicative of the greater variability which occurs in the upper layer of the ocean due to coastal upwelling and evaporation. (In bent sections that begin and terminate at the coast (Figure 2), distance offshore was measured from the end to the south of Monterey Bay, i.e., Kasler Pt., Yankee Pt., and Cypress Pt.).

1. Kasler Pt. to Ano Nuevo

In this section (Figure 10a) negative anomalies of spiciness were found in the upper 100 m in waters greater than 1000 m deep. Over the shelf breaks at both ends of the section, the vertical gradients of spiciness anomalies were weak. The spiciness anomaly was less than -0.28 at stations 52 and 53 at a depth of 80 m. Fronts separated these negative anomalies from positive anomalies which occurred in shallower water. Off Ano Nuevo a shallow feature is found where anomalies are greater than 0.08. At Kasler Pt., a near-surface maximum of 0.08 was found, associated with cold, salty upwelled water. Below 100 m, the general pattern for the section showed relative spiciness maxima over the slope at both ends of the section, indicating the presence of CU water. At Kasler Pt. the spiciness anomaly exceeded 0.08, with two maxima areas between stations 59 and 55 (30 km) vertically centered at 100 (due to upwelling) and 400 m (CU). At the Ano Nuevo side the maximum spiciness anomaly was 0.04 centered along 470 m from 60 to 80 km, but 0.08 at 350 m at station 79. The largest subsurface minima exceeded -0.08 and was centered at 220 m, 50 km offshore.

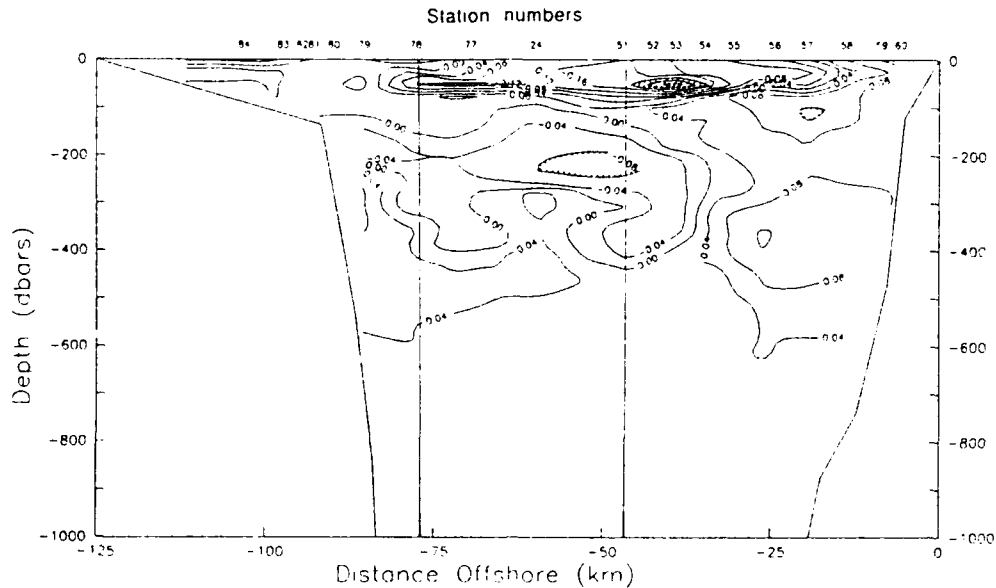


Figure 10a. Kasler Pt. to Ano Nuevo spiciness anomaly: CU shown by subsurface areas of >0.04 spiciness anomaly centered at approximately 300 along continental slope at both ends of section. Distance offshore is measured from Kasler Pt. with vertical lines indicating inflection points of the section.

The density anomaly section (Figure 10b) showed basically level isopycnals in the upper 100 m with a slightly stronger gradient toward Ano Nuevo. Near-surface density decreased offshore indicating an equatorward flow. The pycnocline was deepest in the center of the section near station 51 and shoaled to about 50 m at both ends. Below 200 m, the 26.6 through 27.0 kg/m^3 isopycnals slope down toward Kasler Pt. revealing a northward flow at these depths into the canyon on the Kasler Pt. side. At Ano Nuevo, the 27.0 and 27.2 kg/m^3 isopycnals sloped down at the coast, which is consistent with poleward flow.

2. Yankee Pt. to Santa Cruz

Spiciness anomalies in the Yankee Pt. to Santa Cruz section (Figure 11a) had a pattern similar to the Kasler Pt. section with even greater anomaly values at

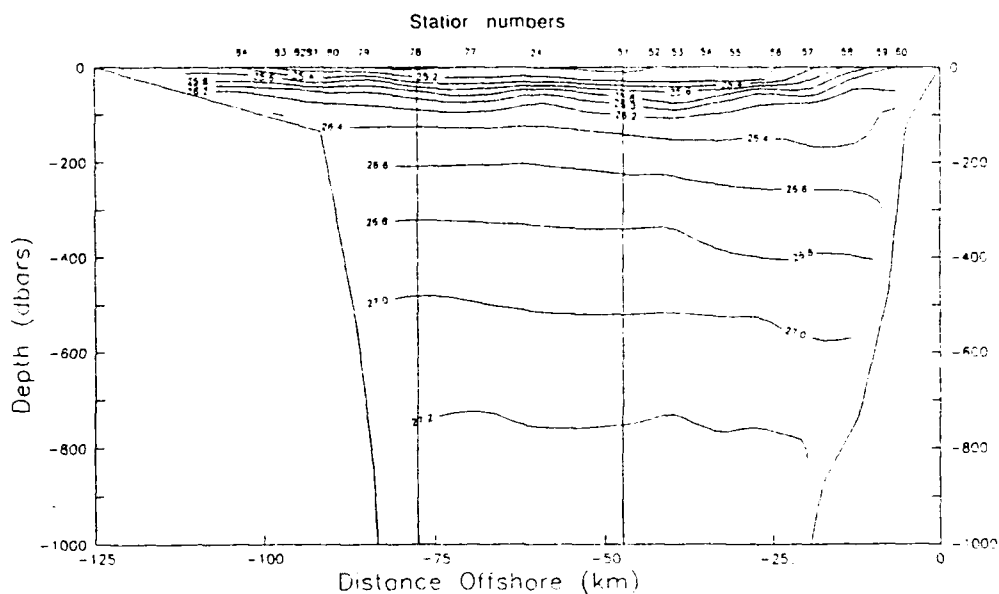


Figure 10b. Kasler Pt. to Ano Nuevo density anomaly: Shoaling isopycnals both ends of the section in the upper 100 m indicated upwelling. The downward sloping isopycnals at Kasler Pt. and Ano Nuevo below 200 m indicated a poleward flowing CU, i.e., into the page at Kasler Pt., and out of the page at Ano Nuevo. Distance offshore was measured from Kasler Pt. with vertical lines indicating inflection points of the section.

the depth of the CU. The water above 100 m had large vertical and horizontal spiciness gradients. The greatest positive anomalies (>0.32) were on the continental shelf at Yankee Pt. and off Santa Cruz at 100 m. Near Yankee Pt. this was caused by coastal upwelling of saltier water, as indicated by the shoaling of isopycnals at the surface (Figure 11b), but at Santa Cruz the isopycnals were relatively level because the temperatures were warmer (Appendix B shows surface temperatures and salinities at station 45 of 10.8°C and 33.7 psu) while inshore at station 42 the values were 11.8°C and 33.7 psu). The minimum

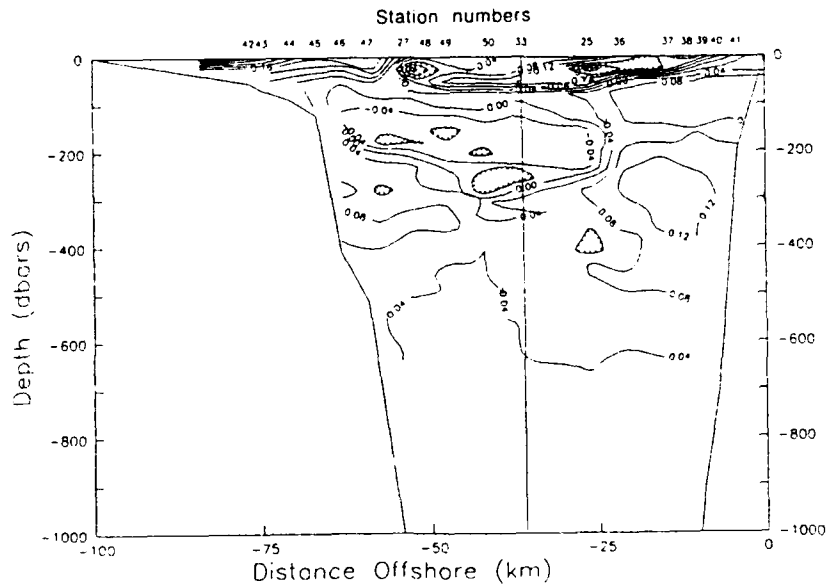


Figure 11a. Yankee Pt. to Santa Cruz spiciness anomaly: CU shown by large positive spiciness anomaly along the continental shelf at a depth of 300 m at Yankee Pt. and 350 m at Santa Cruz. Distance offshore was measured from Yankee Pt. with vertical lines indicating the inflection points of the section.

anomaly (less than -0.24) was found at 50 m depth at station 25 over the axis of the canyon. At the depth of the CU (~300 m) the pattern was also similar to that for Kasler Pt., with an area in the center of the section of negative spiciness anomalies (though this area was smaller and did not extend as deep as the Kasler Pt. to Ano Nuevo section) flanked by positive anomalies associated with the CU. Anomalies near Yankee Pt. exceeded 0.12; the region corresponding to the core of the CU was clearly depicted 20 km offshore and at a depth of 300 m. On the other side of Monterey Bay at Santa Cruz the anomaly exceeded 0.08 with the core of the CU at approximately 350 m extending almost 50 km offshore. In this section the 0.04

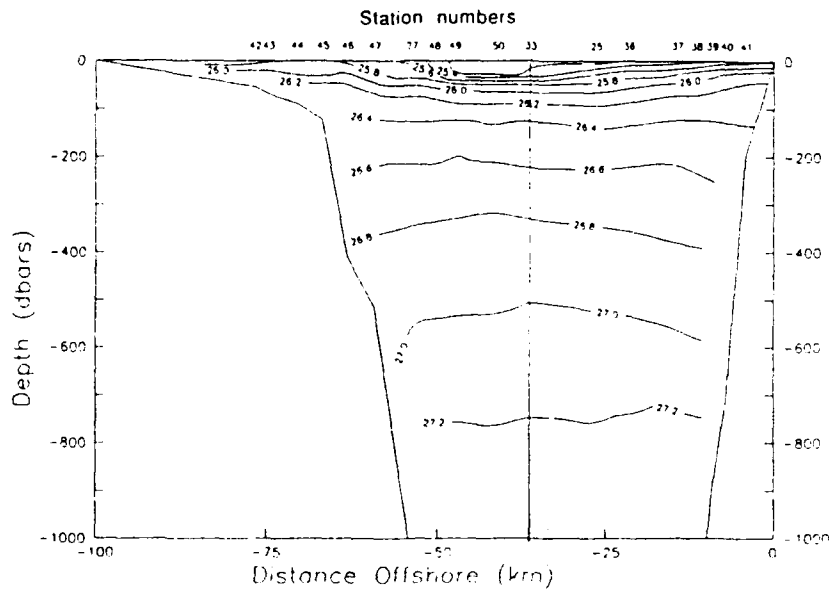


Figure 11b. Yankee Pt. to Santa Cruz density anomaly: Shoaling isopycnals at both ends of the section indicate upwelling of saltier water in the upper 100 m. Below 200 m isopycnals sloped downward toward both shore indicating a poleward flowing CU. Distance offshore was measured from Yankee Pt. with vertical lines indicating the inflection points of the section.

contour extended from one side of the bay to the other, though it shoaled from a depth of 600 m at either end to 400 m at station 50.

The corresponding section of density anomaly (Figure 11b) showed the isopycnals sloping upward from the center of the section to both shores in the upper 100 m. The lightest near-surface water was found at station 50. The vertical density gradient was stronger at the Yankee Pt. end of the section. The 26.4 kg/m³ isopycnal, at approximately 150 m, deepened by about 25 m from Santa Cruz to Yankee Pt. At depths greater than about 200 m (>26.5 kg/m³), isopycnals sloped downward at both ends of the section. The 26.6 kg/m³ contour sloped down very steeply toward Yankee Pt. This was even more apparent in the 26.8 and 27.0 kg/m³ isopycnals at about 400 and 600 m respectively. For the 26.6 to 27.0 kg/m³

isopycnals, the shoalest point shifts southward with depth from station 49 to station 53. At a depth of about 750m, the 27.2 kg/m^3 contour was basically level.

3. Cypress Pt. to Santa Cruz

The spiciness anomalies for the section closest to Monterey Bay are depicted in Figure 12a. Here the upper layer looked much like previous sections with a large positive spiciness gradient at Santa Cruz and an area of spiciness minima (< -0.24) centered at 50 m at station 66. CU water was associated with the $+0.12$ anomaly values at 300 m at each coast, but the area of negative anomalies in the center of the section was absent with the spiciness anomaly contours for 0.04 and 0.08 extending completely across the bay. This indicates that the CU kept the

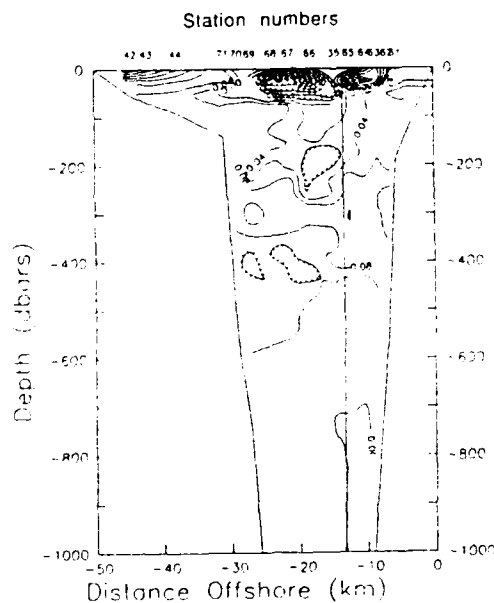


Figure 12a. Cypress Pt. to Santa Cruz spiciness anomaly: Large positive spiciness anomalies which extended across the canyon from Cypress Pt. to Santa Cruz showed the CU flowing perpendicular to the axis of the canyon and poleward at this point. Distance offshore was measured from Cypress Pt. with the vertical line indicating the inflection point of the section.

offshore water from penetrating into Monterey Bay. The distance at a depth of 200 m across the section is less than 25 km. Density anomalies (Figure 12b) looked very much like the Yankee Pt. to Santa Cruz section (Figure 11b) with upward sloping isopycnals at both ends of the section in the upper 100 m. The 26.6 kg/m³ isopycnal was level at 200 m. However, the 26.8 and 27.0 kg/m³ contours only sloped down at Santa Cruz and show a slight upslope at Cypress Pt. The 27.2 isopycnal slopes upward from Santa Cruz to Cypress Pt. (Since there should be no total transport through this section, these deep isopycnal slopes must be due to aliased sampling.)

4. Pigeon Pt. (south)

For the fifth section (Figure 13a), which extends south-southwest from Pigeon Pt., the area of greatest spiciness anomaly in the upper 100 m was found in

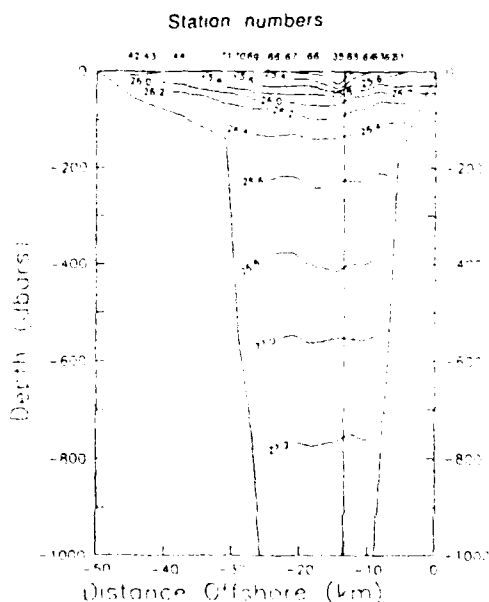


Figure 12b. Cypress Pt. to Santa Cruz density anomaly: Upwelling in the upper 100 m was indicated by the upward sloping isopycnals at both ends of the section. Distance offshore was measured from Cypress Pt. with the vertical line indicating the inflection point of the section.

the vicinity of station 89, where the surface anomaly exceeds 0.22. A small area of maximum negative anomaly was found in the same area at station 88, but at 50 m. Offshore from station 92 at a depth of 75 m is a large area of maximum negative anomalies. No strong positive or negative anomalies were noted below a depth of

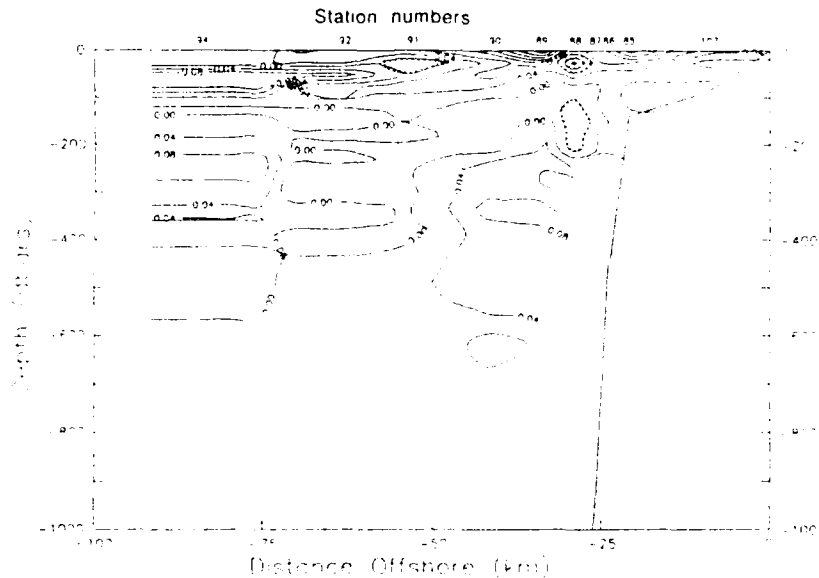


Figure 13a. Pigeon Pt. south spiciness anomaly: CU was shown by the presence of large positive spiciness anomaly area along the continental slope centered at a depth of 350m.

about 100 m and beyond 50 km from shore with the exception of a 0.08 area at 250 m below station 94. Near the coast, where I expect the CU to be found, the maximum spiciness anomaly was centered at approximately 400 m depth and 40 km offshore with values exceeding 0.08. This area extended to a depth of 600 m.

Density anomalies (Figure 13b) looked very similar to the Pt. Sur section (Figure 5c) with a more intense pycnocline observed offshore. The isopycnals sloped upward from station 94 to the coast. The 26.6 kg/m^3 isopycnal, at 200 m, was almost level with a slight downward slope inshore of station 90. Deeper isopycnals sloped downward toward the coast inshore of station 91.

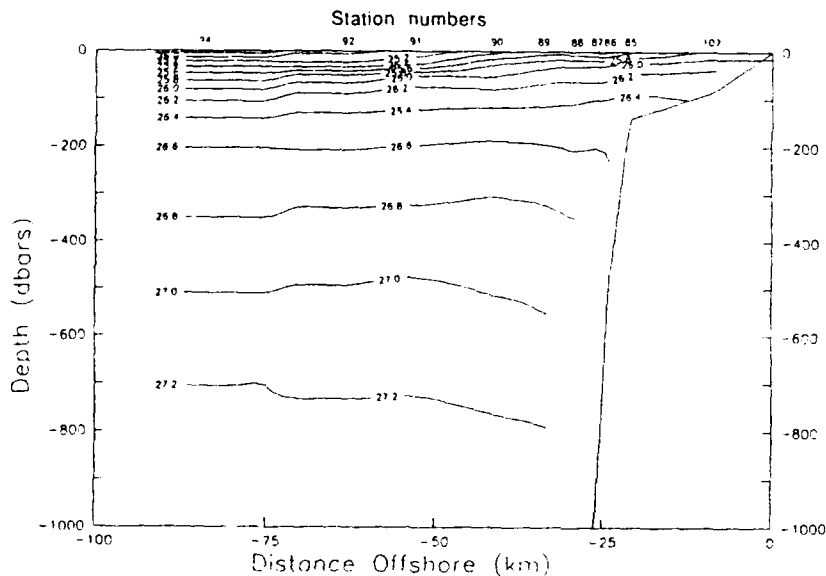


Figure 13b. Pigeon Pt. south density anomaly: Upwelling was observed along the coast as indicated by the shoaling isopycnals in the upper 100 m. The poleward flowing CU was shown by the downward sloping isopycnals below 200 m.

5. Pigeon Pt. (west)

The final section (Figure 14a), which runs to the southwest from Pigeon Pt., showed a pattern of spiciness anomalies in the surface waters very similar to the Pigeon Pt. west section (Figure 13a). A -0.08 area was found at 50 m below station 100, and 0.16 areas at 50 m below stations 97 and 104. Centered about 175 m below station 105 was an area of -0.08 anomaly. Below about 200 m, a larger area of 0.04 anomaly extended from the coast to the offshore end of the section (station 93) and to a depth of 600 m. Within this area was a 0.08 area centered at about 300 m along the continental slope.

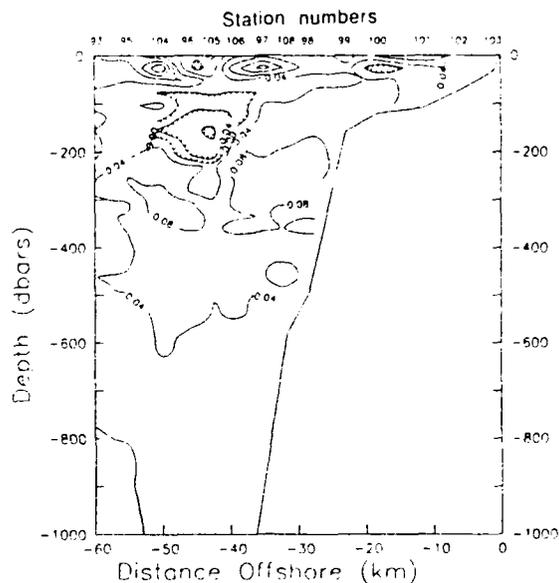


Figure 14a. Pigeon Pt. west spiciness anomaly: The CU was centered at 320 m along the continental slope as indicated by the positive spiciness anomaly.

In the upper 100 m of the water column, the pycnocline (Figure 14b) was markedly different than previous sections; it was most intense at the continental shelf break (station 99) instead of offshore. The 26.6 and 26.8 kg/m^3 isopycnals sloped upward from the offshore end of the section to station 98 then sharply slope downward into the coast. At a depth of 550m the 27.0 kg/m^3 isopycnal showed some undulation, but still sloped downward towards the coast, as did the 27.2 kg/m^3 at 800 m.

6. Summary

All six sections of spiciness anomalies (Figures 5e, 10a, 11a, 12a, 13a, and 14a) exhibit a similar pattern. 1) In the upper 100 m, variability was large with negative anomalies in regions of deep water (CC) and positive anomalies over the

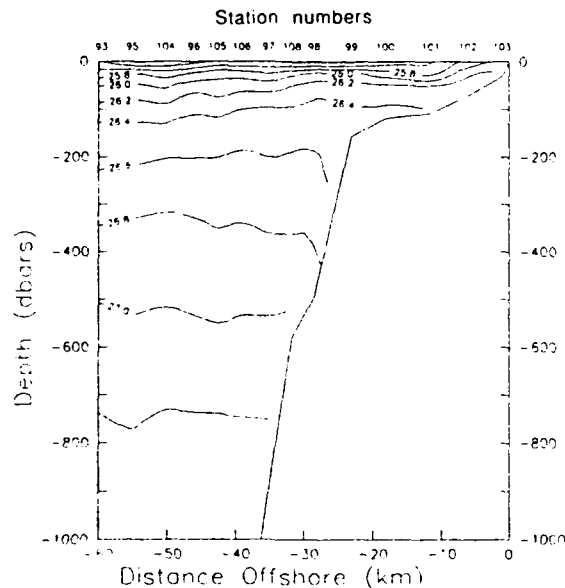


Figure 14b. Pigeon Pt. west density anomaly: Upward sloping isopycnals showed coastal upwelling in the upper 100 m and downward sloping isopycnals showed poleward flow below 200 m.

continental slope (upwelled water). 2) A very sharp gradient of spiciness, or "spicecline", was observed at a depth of about 100 m separating upper and lower waters. 3) From 100 m to about 600 m, negative anomalies occurred in the center of the study area and areas of positive anomalies (0.08) occurred closer to shore along the continental slope. It is these areas of positive anomalies (warm, salty water) that indicate the presence of the California Undercurrent.

Similarities also existed in the patterns of isopycnals for the six sections (Figures 5c, 10b, 11b, 12b, 13b, and 14b). 1) The upper layers showed the pycnocline extending to about 100 m with the isopycnals generally sloping upward

towards the shore. 2) From 100 m to about 200 m the isopycnals still sloped upward towards the shore, but the slope was gentler with a much weaker vertical gradient of density anomaly than in the surface layer. 3) Below about 200 m the shape of the isopycnals reversed with a doming in the center of the study area and downward sloping towards the shore. The areas of downward sloping isopycnals near the continental slope implied poleward flow and hence the presence of the California Undercurrent.

Comparing the sections of spiciness anomalies to the sections of density anomaly shows that the area of highest subsurface spiciness anomalies were found between the 26.6 and 26.9 kg/m³ density anomaly surfaces.

D. HORIZONTAL CHARTS OF SPICINESS ANOMALY AND DENSITY ANOMALY DEPTHS

As the density layers chosen by Lynn and Simpson (1989) correlated well with observed layers of spiciness anomalies off Monterey, I chose these density layers to examine the pattern of horizontal variability of spiciness anomalies. The values of spiciness anomaly are averaged between upper and lower boundaries of density anomaly to avoid patchiness associated with fine scale intrusions. One extra layer was added below the lowest layer used by Lynn and Simpson (1989).

The density anomaly levels between 25.6 and 26.0 kg/m³ represent the upper layer and is centered at about 50 m. The characteristics of the water in this layer are affected by several processes, including coastal upwelling, winter storms, seasonal heating, air-sea exchanges and runoff. Layer 2 contains density anomaly levels from 26.0 to 26.4 kg/m³ and extends from approximately 50 m to 150 m. In this layer coastal upwelling still affects the characteristics of the water, but not as strongly as in Layer 1. The lower half of this layer is also where I observed the

intrusion of isohaline layer offshore along the Pt. Sur section. (This isohaline layer is subducted from higher latitudes.) Layer 3 includes density anomaly values from 26.4 to 26.6 kg/m³ and is centered at approximately 200 m. In this layer, and below, the effect of coastal upwelling is no longer present and variations in the water mass characteristics are caused entirely by lateral mixing and transport. Layer 4 extends from a density anomaly 26.6 to 26.9 kg/m³ which corresponds to depths of approximately 225 m to 500m. Layer 5 includes density anomaly levels from 26.9 to 27.1 kg/m³ corresponding to depths of approximately 500 and 700 m respectively.

Horizontal charts were also made of depth corresponding to the density anomaly levels at the center of the five layers of density anomaly.

1. Layer 1: 25.6-26.0 kg/m³ γ_{θ}

As this layer is very close to or at the surface, one would not necessarily expect to find Undercurrent waters. An area of greater than 0.08 anomaly was found southwest of Pigeon Pt. approximately 30 km offshore (Figure 15a) where temperatures and salinities were both slightly higher. A very large area of negative spiciness anomalies was found approximately 20 km west of Cypress Pt. with values less than -0.12. Here surface temperatures were similar to those offshore, but salinities were slightly fresher. Anomalies were also positive in Monterey Bay, so a very strong gradient of spiciness anomalies with contours running north/south was present at the edge of the bay.

The depth of the 25.8 kg/m³ density anomaly contour was deeper offshore (greater than 60 m) and shallower near the coastline (less than 20 m) (Figure 15b). A fairly continuous 30 m contour ran along the coast from Pt. Sur north to Ano Nuevo where it turned and proceeded to the southwest. The 40 m

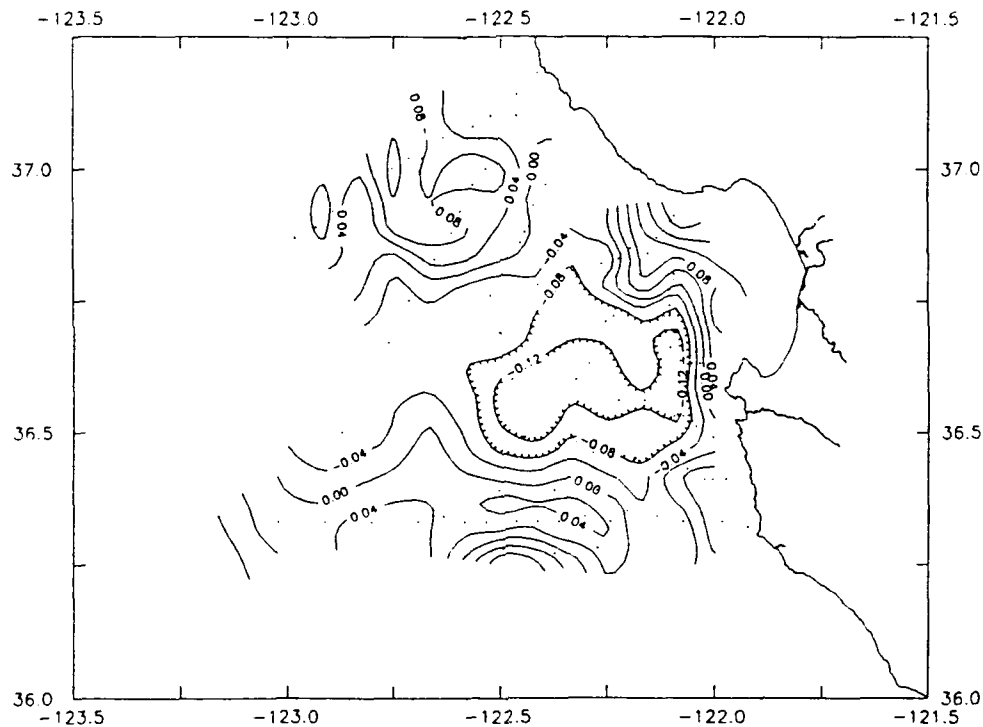


Figure 15a. Spiciness anomaly averaged over 25.6-26.0 kg/m³ density anomaly layer: A large area of negative spiciness anomaly in the upper 100 m was observed with strong gradients near the mouth of Monterey Bay. The depth of this layer was centered at about 50 m.

contour paralleled the 30 m contour until it crossed the deepest part of the canyon, then diverged toward the west. The 50 m contour paralleled the coast, but far offshore, in the vicinity of station 16, looped towards the bay as it neared station 92, entering as close as station 55 before heading back out to sea. A deep maximum was found west of Yankee Pt. in the vicinity of station 52 with depths exceeding 60 m. A large shallow minimum was found southwest of Pigeon Pt. centered between stations 87 and 98 where the isopycnal was shallower than 20 m.

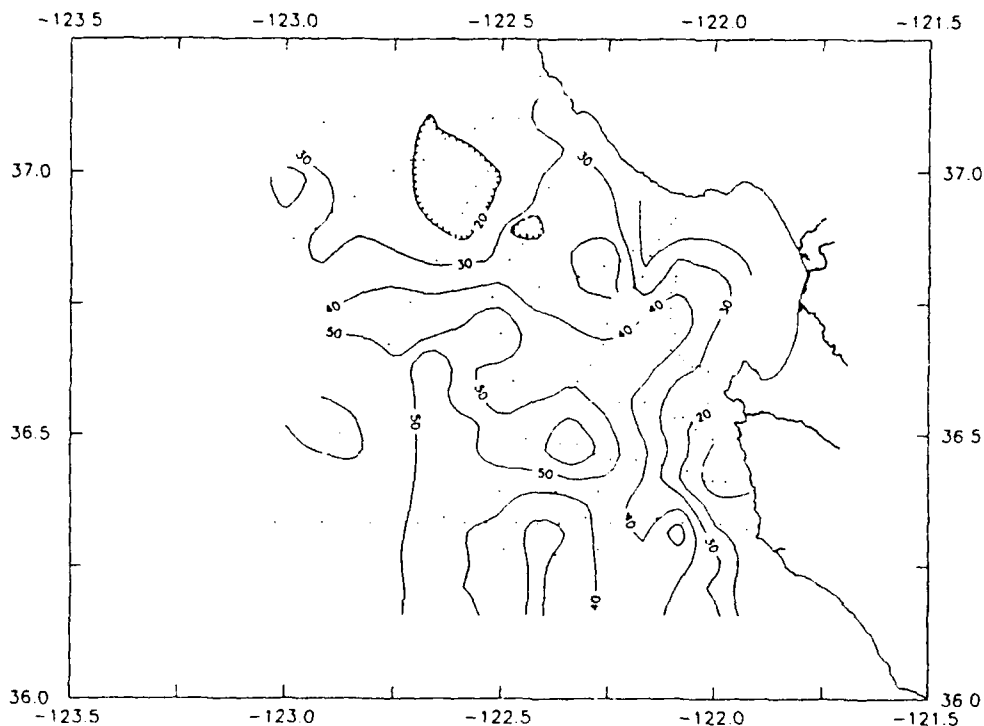


Figure 15b. Depth of 25.8 kg/m^3 isopycnal: An offshore trough and shoaling isopycnals indicated anticyclonic or equatorward flow in the surface layers.

2. Layer 2: $26.0\text{-}26.4 \text{ kg/m}^3 \gamma_\theta$

Layer 2 (centered at about 100 m) showed much less variation in spiciness anomalies (Figure 16a). The 0.04 contour followed the coast as in Layer 1, but moved farther out to sea as it ran around an area of 0.08 anomaly (west of Carmel Bay) where surface temperatures and salinities were slightly warmer and saltier than offshore. The other areas of large positive or negative noted in Layer 1 were absent as was the strong gradient near Monterey Bay.

The general pattern of the depth of 26.2 kg/m^3 isopycnal (Figure 16b) was similar to 25.8 kg/m^3 , that is shallower towards the coast. The 80 m contour ran to the north 30 km off Pt. Sur paralleling the coast, then turned for a short

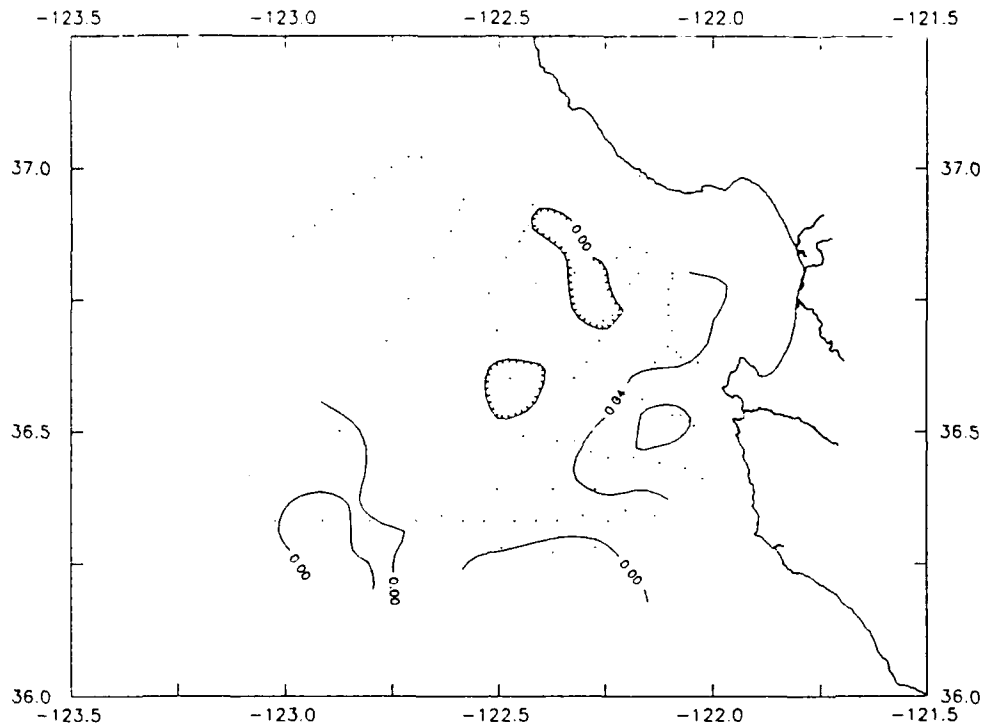


Figure 16a. Spiciness anomaly averaged over 26.0-26.4 kg/m³ density anomaly layer: The positive anomaly of spiciness observed paralleling the coast indicated the location of the CU between approximately 50 to 150 m. The depth of this layer was centered at about 100 m.

excursion into the bay over the center of the canyon before reversing direction to parallel the north wall of the canyon. Nearing station 49 it turned sharply toward shore, rounded station 74 and headed out towards station 91. Strongest gradients were observed in the vicinity of station 74. Past Ano Nuevo and Pigeon Pt., the gradients relax greatly from the 80 m contour offshore to the nearshore 50 m contour. The deep maximum was still found west of Yankee Pt. with depths greater than 100 m, but the shallow minimum found at the 25.8 kg/m³ isopycnal seen 30 km offshore of Pigeon Pt. was then observed at the coast.

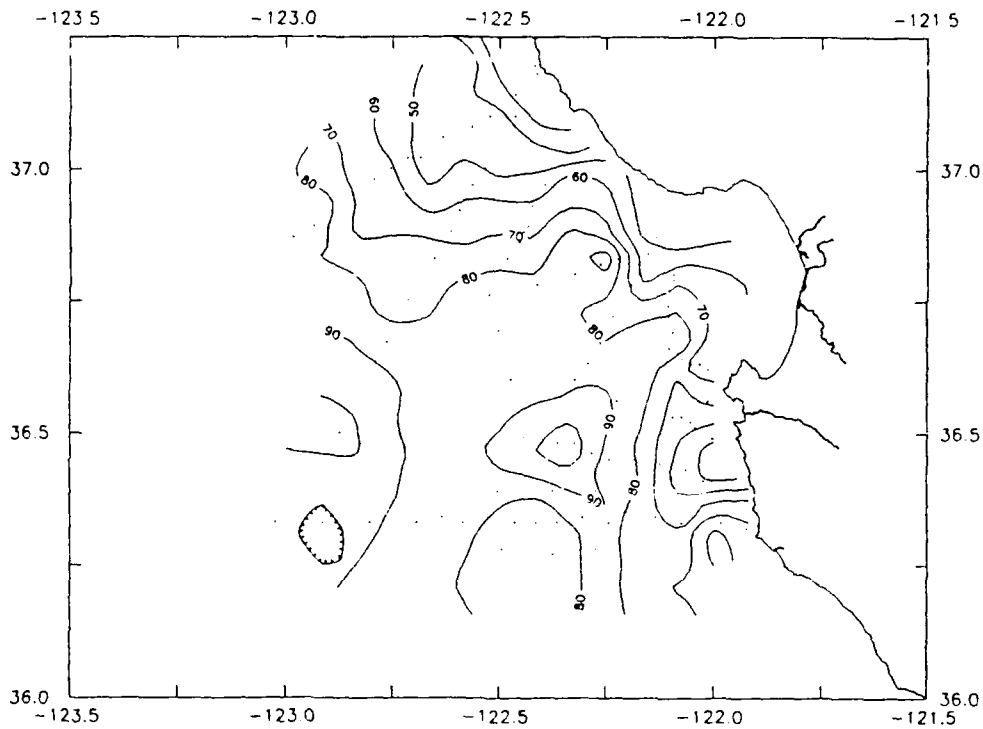


Figure 16b. Depth of 26.2 kg/m^3 isopycnal: A troughing of the isopycnal offshore was observed indicating anticyclonic flow. The strongest gradients near the coast indicated the greatest flow.

3. Layer 3: $26.4\text{-}26.6 \text{ kg/m}^3 \gamma_\theta$

In this layer, at a depth of approximately 200 m, the 0.04 spiciness anomaly contour was continuous from Pt. Sur (25 km offshore) all the way past Pigeon Pt. (40 km offshore) (Figure 17a). Greater positive spiciness anomalies were found near the coast. As with layer 2, the spiciness anomaly gradients were much weaker than in layer 1 indicating more uniform water characteristics. Again, to the west of Carmel Bay the contour ran offshore around a small area of 0.08 anomaly before moving closer (10 km) to shore, where the water was both warmer and saltier than offshore. There was a -0.04 anomaly 30 km west of Cypress Pt. the size of Monterey Bay, where the water was slightly cooler and

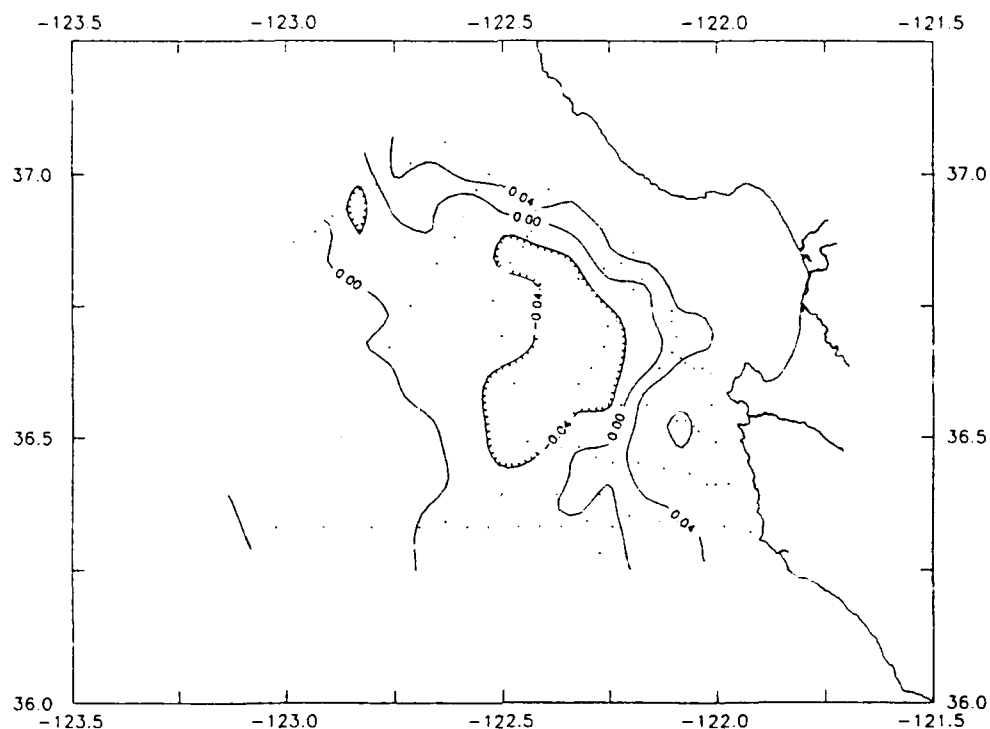


Figure 17a. Spiciness anomaly averaged over 26.4 - 26.6 kg/m³ density anomaly layer: Increased positive anomalies of spiciness observed near the coast showed stronger indications of the CU between 150 and 225 m.

fresher than offshore.

The depth of 26.5 kg/m³ isopycnal (Figure 17b) was still similar to the two upper levels, with the greatest depths offshore and isobaths roughly paralleling the coast. Three deep maxima (>210 m) were observed off Carmel Bay. A trough extended onshore off Kasler Pt. then north and into Monterey Southwest of Santa Cruz, the 130 to 160 m isobaths paralleled the coast with the shoalest area adjacent to Pigeon Pt.

4. Layer 4: 26.6-26.9 kg/m³ γ_{θ}

This layer extends from 225 to 500 m. The characteristic signature of larger positive spiciness anomalies was stronger than in the layers above (Figure

18a). The contours still basically followed the coastline. However the gradient between the contours has relaxed somewhat with the 0.04 contour now located further offshore and the 0.08 contour located approximately where the 0.04 contour was in layer 3. Near the head of the canyon, the spiciness anomaly reaches over the 1000 m isobath, then decreases showing no presence of the CU over the 200 m isobath.

At the level of the 26.7 kg/m^3 density anomaly (Figure 18b) the pattern of the isobaths has begun to reverse from the previous three levels. The depths now

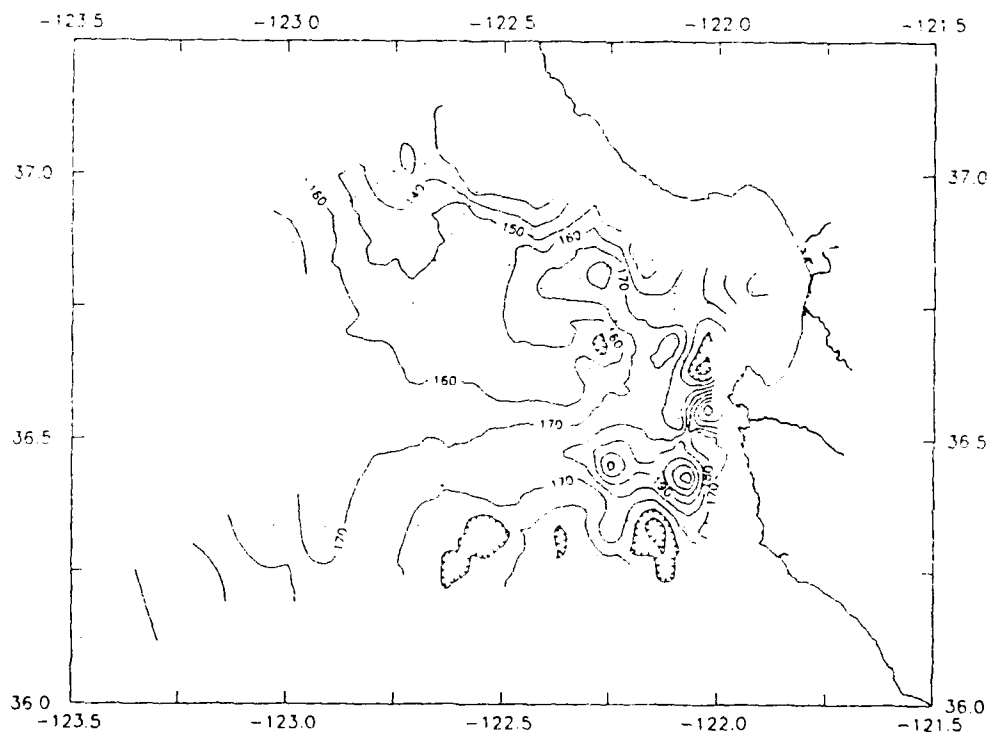


Figure 17b. Depth of 26.5 kg/m^3 isopycnal: A deep trough extended towards Monterey Bay from offshore with shoaling of the isopycnal surface near the coast. At the head of the canyon, the isopycnal surface deepened towards the coast.

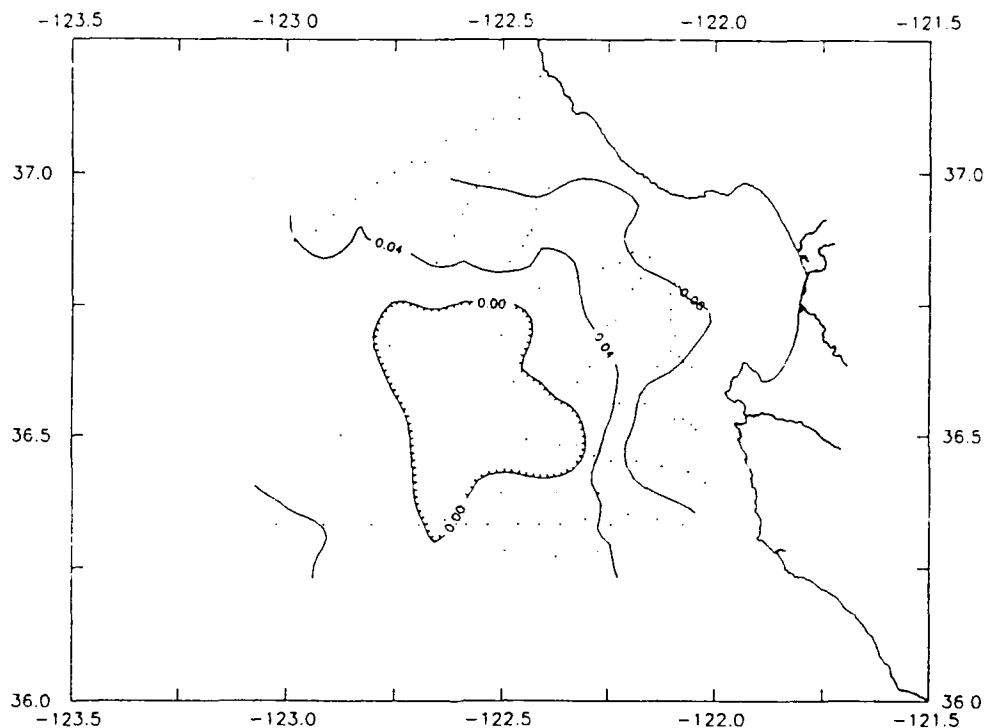


Figure 18a. Spiciness anomaly averaged over 26.6 - 26.9 kg/m³ density anomaly layer: Between depths of 225 and 500 m the strongest signature of the CU in terms of spiciness anomaly was present. The largest positive anomalies were observed near the shore.

increase from an average depth of 260 m or less offshore to greater than 320 m at the deep maximum to the west of Kasler Pt. near station 55. In the vicinity of this deep maximum the depth contours were tightly packed and almost create a closed bull's-eye. Across the mouth of Monterey Bay the depth gradient was relatively strong with a depth of 310 m at the mouth and 270 m reached 20 km to the west.

With the exception of the area to the west of Monterey Bay, most contours did not parallel the coast. A shallow minimum appeared southwest of Pigeon Pt. at station 90 with depths less than 240 m. Over the head of the canyon the depth of the isopycnal increased toward the coast to greater than 340 m at station 30.

5. Layer 5: 26.9-27.1 kg/m³ γ_{θ}

At this depth the spiciness anomalies were still greater near the coast (Figure 19a), but this pattern was not as strong as at Layer 4 and gradients were weaker throughout the area. Compared to Layer 4, the 0.04 contour at Layer 5 moved onshore at Pt. Sur (25 km offshore), and farther offshore to the west of Carmel Bay (45 km), then returned to a point 10 km off Cypress Pt. It then proceeded towards the northwest past Pigeon Pt. at about the same distance offshore as Layer 4 taking the same excursion towards the shore between Santa Cruz and Ano Nuevo. Near the end of the canyon, spiciness anomaly values exceeding 0.08 were found.

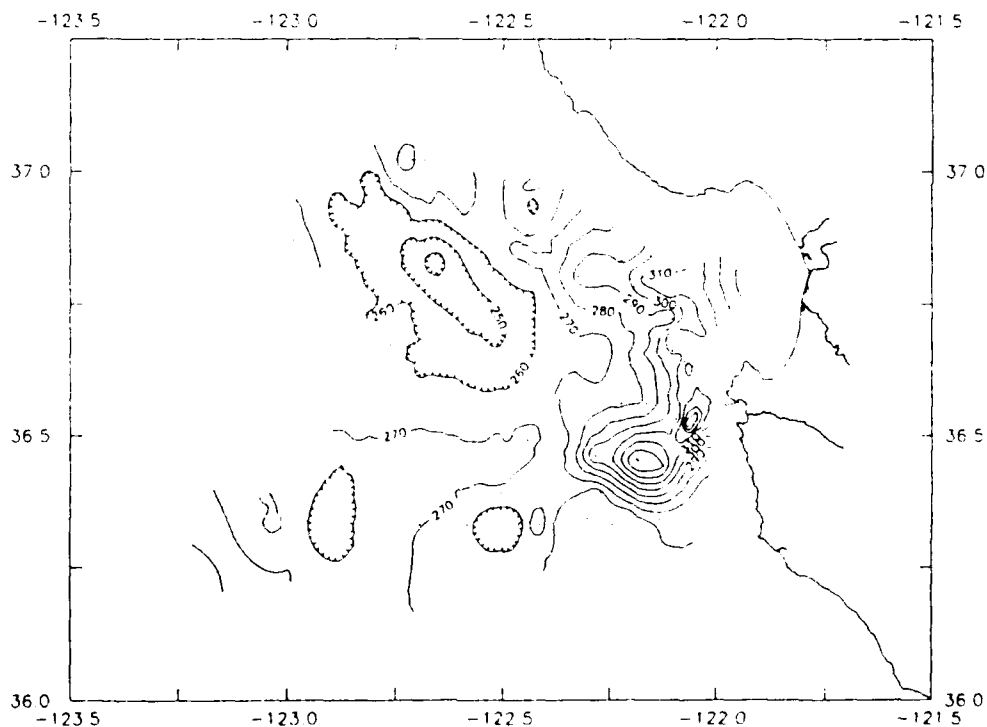


Figure 18b. Depth of 26.7 kg/m³ isopycnal: Strong gradients were observed off Carmel and Monterey Bays indicating the areas of strongest flow

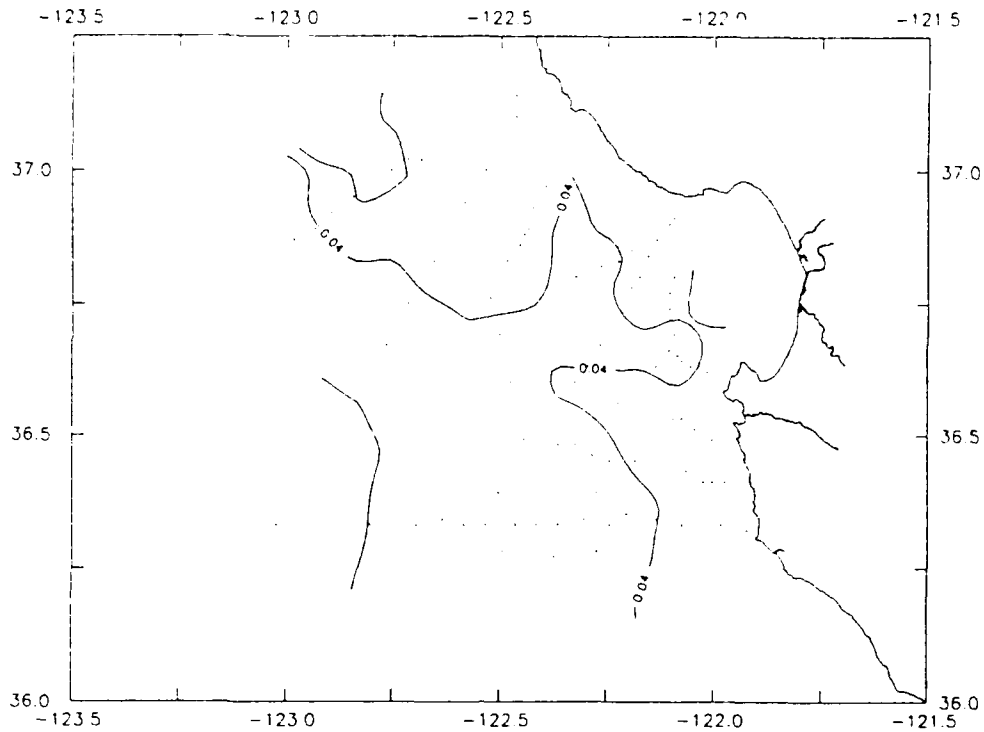


Figure 19a. Spiciness anomaly averaged over $26.9 - 27.1 \text{ kg/m}^3$ density anomaly layer: The presence of CU water (marked by the 0.04 contour) was observed at these depths (500 to 700 m) by the positive spiciness anomalies near the coast.

The depth of deepest density anomaly level, 27.0 kg/m^3 , is shown in Figure 19b. The overall pattern was similar to that observed at the 26.7 kg/m^3 level with isobaths generally deepening toward the coast. However, the deep maximum that was seen at all other levels to the west of Yankee Pt. disappeared and was replaced by evenly spaced contours with depths varying from 500 m offshore to 560 m near the coast along the Pt. Sur transect. The 520 and 530 m contours were the only two which can be easily followed from the Pt. Sur section along the coast through the Pigeon Pt. (west) section. At the Pt. Sur section they were about 40 km offshore, and maintained approximately the same distance past Kasler and

Cypress Pts. Here they turned to parallel the coast past Santa Cruz at a distance of about 45 km from shore increasing to over 50 km offshore from Pigeon Pt. The shallow minimum that appeared to the southwest of Pigeon Pt. at 26.7 kg/m^3 density anomaly moved slightly to the east. The 27.0 kg/m^3 isopycnal sloped down toward the coast from south to north near the end of the canyon indicating a westward flow along the north wall.

F. CHARTS OF DYNAMIC HEIGHTS

From the discussion of results of Pegasus velocity measurements (Figures 6a, 6b, 7a, and 7b), it was clear that selecting a level of no motion at 500 m, as done in

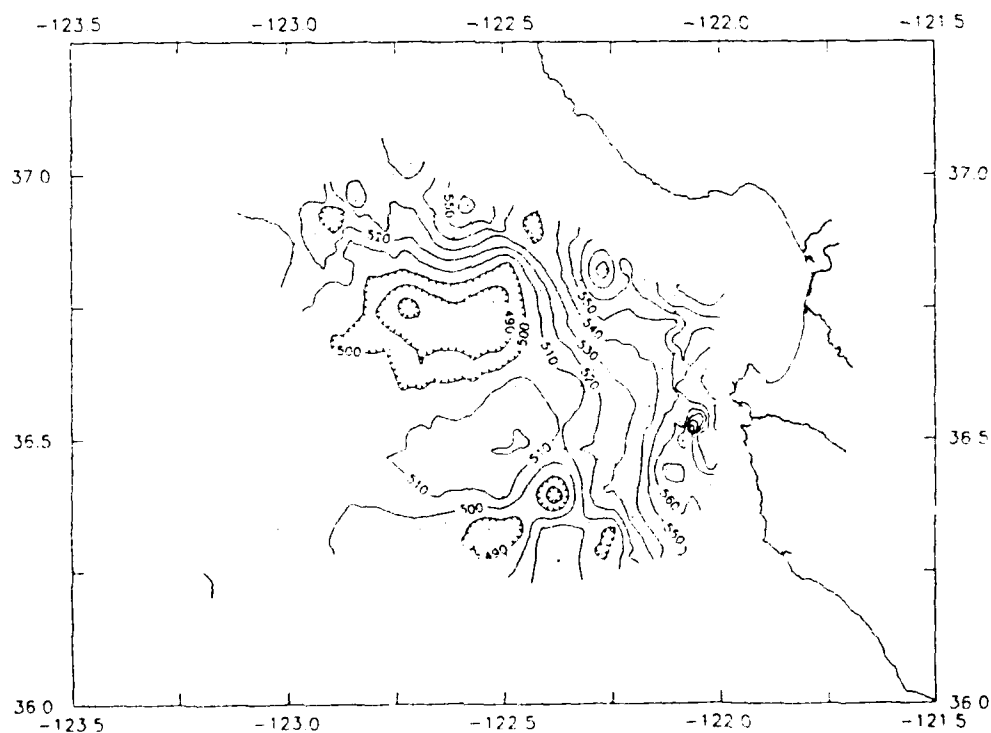


Figure 19b. Depth of 27.0 kg/m^3 isopycnal: A ridge extended towards the shore with strong horizontal gradients observed paralleling the coast in the vicinity of the 1000 m isobath (Figure 1) indicating poleward flow.

previous studies, was incorrect. A choice of 2400 m would be more appropriate. But as only 21 of our 110 stations exceeded 2400 m, and 500 m was a useful reference for previous studies, I discuss two charts of dynamic height using a 500 dbar reference level. However the potential bias due to this choice of reference level must be kept in mind.

1. 0/200

At a depth of 200 dbar (Figure 20a), the isopycnals were relatively level (Figures 5c, 10b, 11b, 12b, 13b, and 14b) so 200 dbar was used as a reference level to examine near-surface flow patterns. A ridge extended onshore towards Monterey Bay with a high located 50 km off Kasler Pt. A continuous equatorward flow was indicated by the largest gradients over the 1000 m isobath (Figure 1)

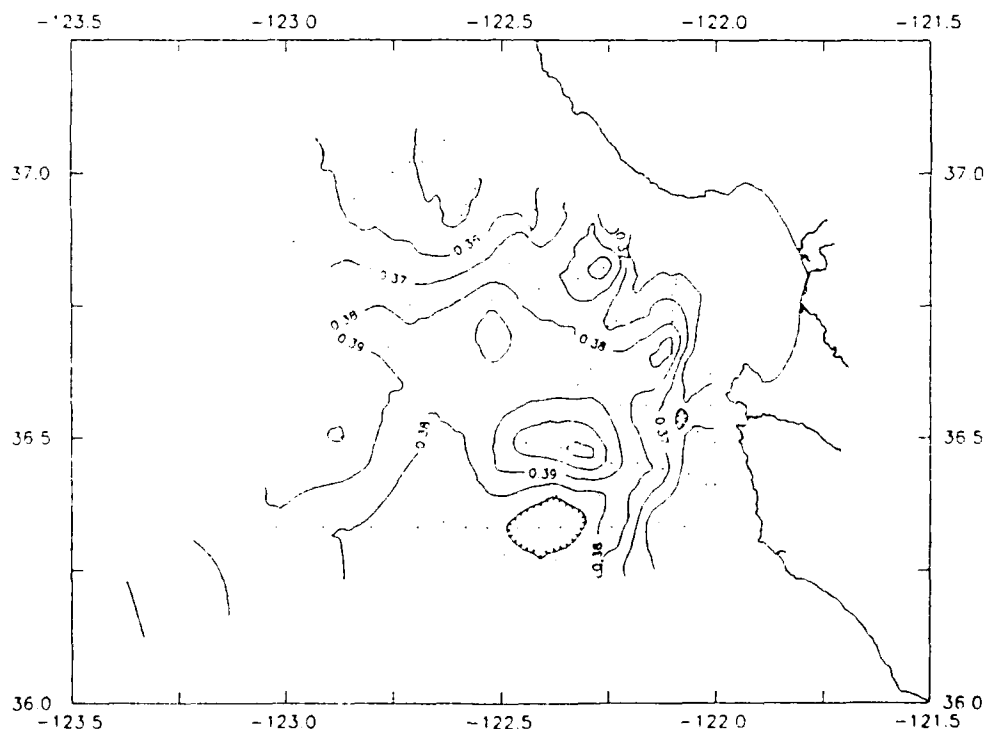


Figure 20a. Dynamic heights at surface referenced to 200 dbar: A dynamic ridge was observed extending onshore south of Monterey indicating anticyclonic flow. The largest gradients were seen near the coast near the 1000 m isobath.

from Pigeon Pt. past Pt. Sur. Maximum velocities in this region were approximately 50 cm/s off Pt. Sur, 75 cm/s west of Cypress Pt., and 20 cm/s southwest of Ano Nuevo. Heights decreased towards Monterey Bay.

2. 0/500

The dynamic heights at the surface referenced to 500 dbar (Figure 20b) closely resembled the 0/200 dbar pattern (Figure 20a). A ridge extended from the mouth of Monterey Bay west to 123° W with a maximum dynamic height of 0.80 dyn m. A low of 0.74 dyn m was observed southwest of Pigeon Pt. As with the 0/200 pattern, heights in Monterey Bay decreased towards the shore. Typical geostrophic velocities were approximately 50 cm/s west of Kasler Pt., 75 cm/s off

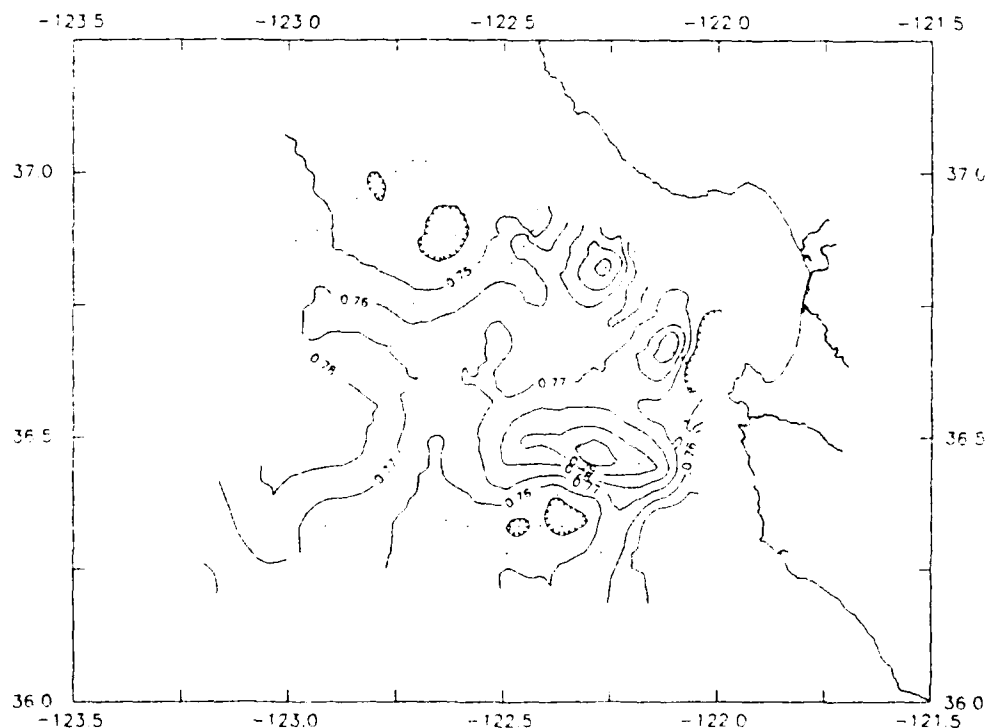


Figure 20b. Dynamic heights at surface referenced to 500 dbar: A dynamic ridge was observed extending onshore indicating an anticyclonic flow as when a 200 dbar reference level was used (Figure 20a).

Cypress Pt. and 20 cm/s southwest of Ano Nuevo. The geostrophic flow pattern associated with these features would advect water into the bay from the north and out of the bay to the south..

3. 200/500

The dynamic heights at 200 m referenced to 500 dbar provide a completely different picture of the flow pattern (Figure 20c). Here, the heights decreased seaward from Pt. Sur to Pigeon Pt. Over the canyon, the heights deepened toward Moss Landing. The maximum gradient was found approximately

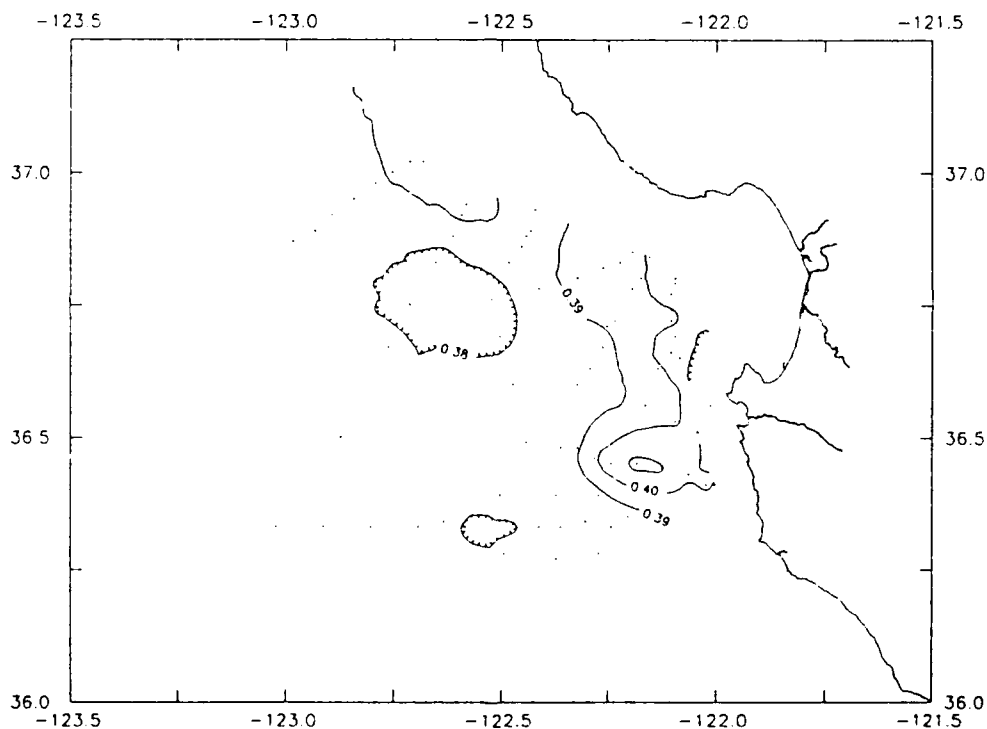


Figure 20c. Dynamic heights at 200 m referenced to 500 dbar: The largest gradient of dynamic heights were observed paralleling the coast in the vicinity of the CU. Dynamic heights deepening towards shore were indicative of poleward flow.

30 km west of Yankee Pt. (30 cm/s geostrophic velocity), corresponding to the positive spiciness anomaly observed in Layers 2 and 3 (Figures 16a and 16b). The largest horizontal height gradients were observed paralleling the coast in the region of the CU with the remainder of the area being relatively homogeneous. Geostrophic velocities were weaker than in the surface layers (Figures 20a and 20b); 25 cm/s off Kasler Pt., 15 cm/s off Cypress Pt., 5 cm/s southwest of Santa Cruz, and 15 cm/s southwest of Ano Nuevo. Forty km southwest of Ano Nuevo, a dynamic trough of 0.38 dyn m was observed.

G. HORIZONTAL CHART OF SALINITY AT CORE OF THE CU

A comparison of the vertical sections of spiciness anomalies and density anomaly showed the area of maximum spiciness anomalies below the surface corresponding to an average density anomaly of approximately 26.7 kg/m^3 . I will assume that this isopycnal gives the best representation of the core of the CU (Figures 5c, 5e, 10a-14b).

The chart of salinity on the 26.7 kg/m^3 density anomaly level (Figure 21a) shows a clear pattern of more saline water (>34.16 psu) near the coastline (the CU) and less saline water (<34.12 psu) offshore. Isohalines generally paralleled the coastline with the 34.16 psu isohaline remaining continuous from Pt. Sur, where it was approximately 30 km offshore, past Pigeon Pt., where it was over 40 km offshore. It was nearest to the coast off Santa Cruz (<10 km). The center of the study area was also dominated by an area of fresher water, where closed isohalines of 34.12 to 34.08 psu make an almost box-shaped 30 km square feature centered at station 24. Over the canyon, the salinity increased onshore to a maximum at the 1000 m isobath, then decreased near the 200 m isobath.

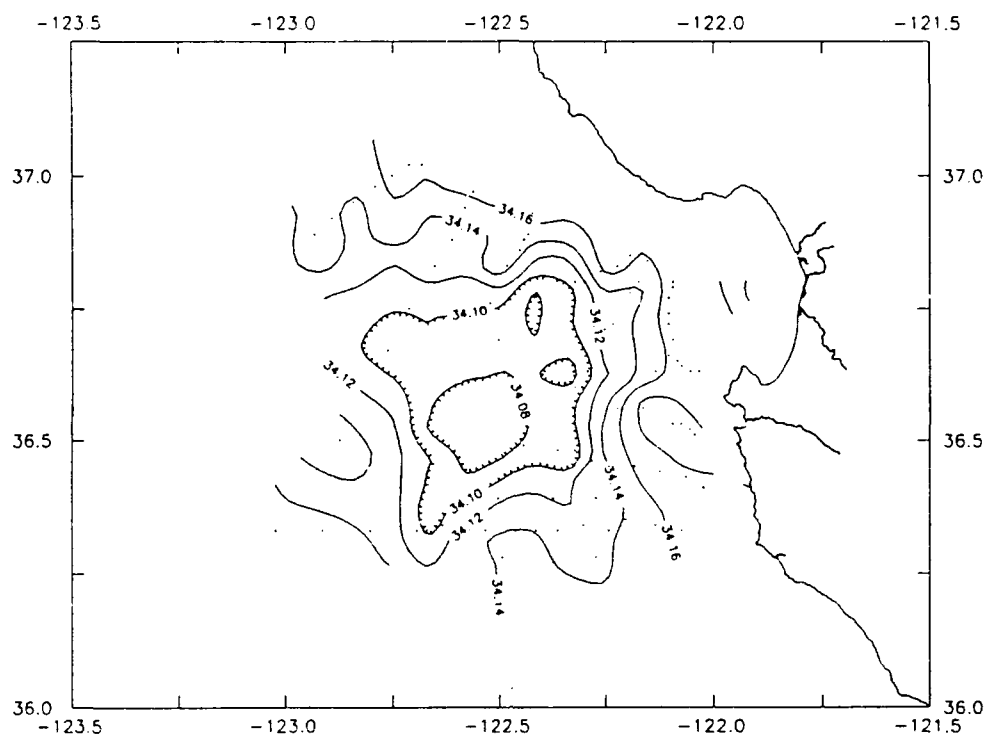


Figure 21a. Salinity at 26.7 density anomaly level: Salinities greater than 34.16 psu were observed in the region of the CU.

H. AVHRR AND SST IMAGERY

Sea surface temperatures for 24 May are shown in the AVHRR image (Figure 22). Upwelling was observed off Pt. Sur as indicated by the area of colder water ($<10^{\circ}\text{C}$) which extends almost 60 km off the coast, where surface temperatures increased to approximately 13°C . Upwelling was also seen to the west of Ano Nuevo (11 to 10°C), with cooler water between Cypress Pt. and Santa Cruz (12 to 13°C). The warmest values were seen offshore approximately 100 km west-southwest of Monterey Bay ($>15^{\circ}\text{C}$). Surface temperatures were approximately 14°C over the rest of the study area, including over the shelf of Monterey Bay. The presence of warmer water in the center of the study area was indicative of anticyclonic flow at the surface.

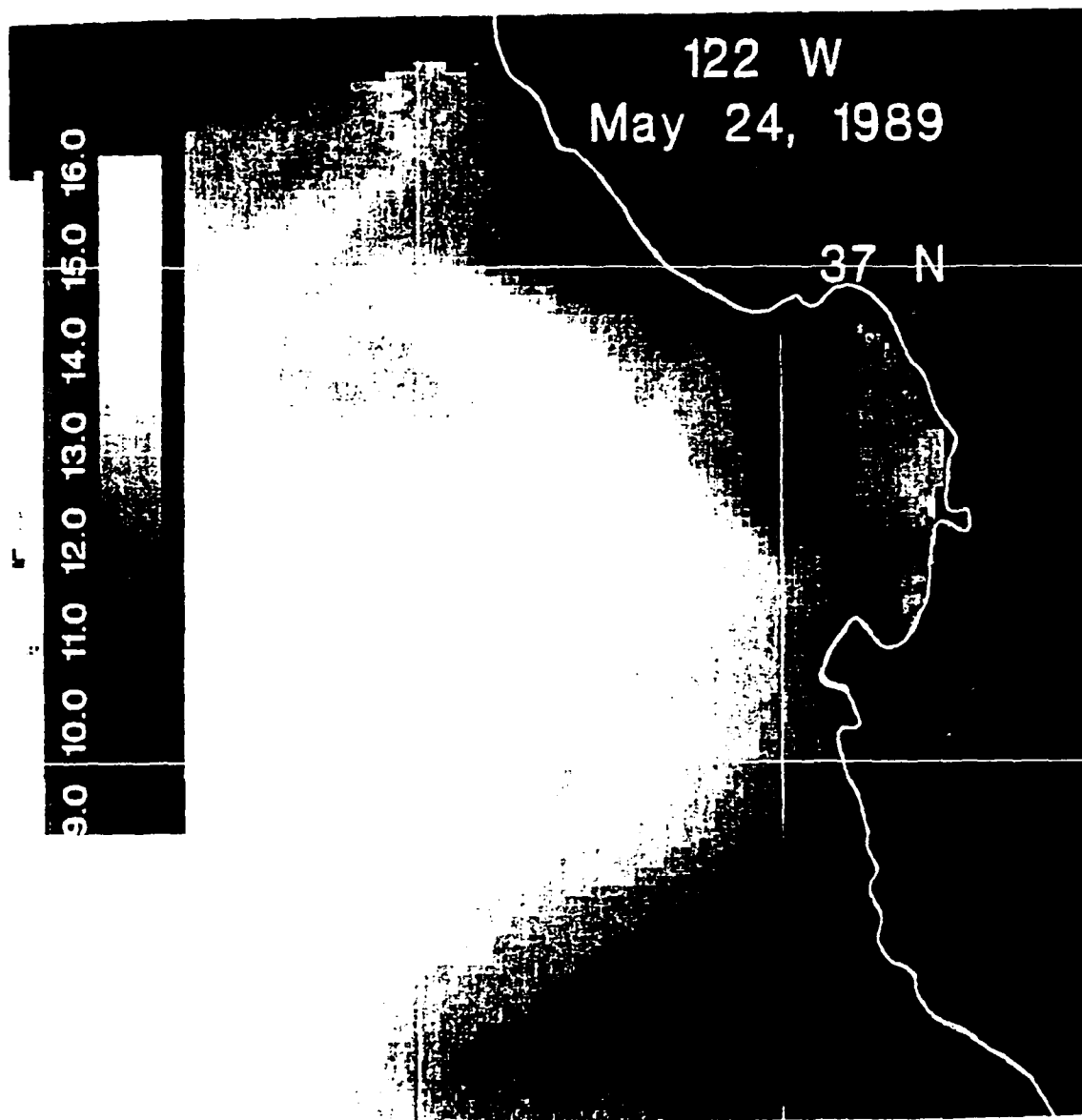


Figure 22. AVHRR SST imagery for 24 May 1989: Upwelling of colder (dark) water was observed at Pt. Sur, which extended approximately 60 km seaward, and along the coast between Santa Cruz and Pigeon Pt. Warmer water (white) observed offshore indicated anticyclonic flow.

IV. DISCUSSION

A. PATH AND FLOW OF CALIFORNIA UNDERCURRENT

1. Identification of California Undercurrent

The region of the CU can be identified in three ways, 1.) by actual direct observations of poleward flow, 2.) by poleward flow inferred from horizontal pressure gradients through geostrophic equilibrium, or 3.) by water mass analysis. Water mass analysis compares temperature and salinity characteristics for a given hydrographic station to waters of equatorial and subarctic origin. The CU is identified as subsurface water of equatorial origin that is warmer and saltier than offshore CC water of subarctic origin at the same density (Lynn and Simpson 1989). These CU waters exhibit a positive anomaly of spiciness. This subsurface positive spiciness anomaly lies between the 26.6 and 26.9 kg/m³ density anomaly levels.

Geostrophically, the CU also has a dynamic signature. This consists of isopycnals at depths greater than 200 m which slope downward at the coast. Along a geopotential (or level) surface, this implies less dense water at the coast. Geostrophy requires that this horizontal pressure gradient be balanced by poleward flow. The more intense this downwelling of isopycnals, the stronger the poleward flow.

Off Pt. Sur, currents were measured directly using Pegasus. Pegasus north/south velocity sections (Figures 6a and 6b) show a poleward flow from the shore to a distance of almost 100 km extending from the surface to a depth of 800 m. At 75 km offshore, the depth of the poleward flow increases to a depth of 2000

m and this level of no motion extends to the coast. Highest speeds (>20 cm/s) were observed at the station closest to the shore (30 km). An equatorward jet (10 cm/s) was located at the surface 75 km offshore.

Clearly the patterns of spiciness and its anomaly disagreed with the isotachs in Figures 6a and 6b. The spiciness anomaly greater than 0.04 represents only a relatively narrow layer between 200 and 400 m corresponding to poleward velocities greater than 2 cm/s. Yet as a tracer, and in an average Lagrangian sense, spiciness anomaly must represent the core of the CU waters.

Our final indicator of the CU, downwelling isopycnals (Figure 5c), better represented the total depth of the poleward flow but was much noisier. The ridge in the isopycnals, which occurred about 75 km offshore between density anomaly surfaces of 26.6 and 27.2 kg/m^3 , corresponded to the spiciness anomaly greater than 0.04 between density anomaly surfaces 26.6 to 26.8 kg/m^3 , and a poleward velocity greater than 2 cm/s. The band of velocities from 10 to 16 cm/s which occur 30 to 40 km from the coast was also marked by downwelling isopycnals. Dynamic height produced strong vertical bands (Figure 9) with more reversals of flow than observed with Pegasus. This noise was attributed to internal waves and difficulties in applying geostrophy in coastal areas.

With these limitations in mind, I describe the path of the California Undercurrent off Monterey using the above mentioned indicators.

2. Spiciness anomaly

The positive anomaly of spiciness between the 26.4 to 26.6 kg/m^3 isopycnal layer (Figure 17a), centered at a depth of about 200 m, clearly showed the CU paralleling the coast from Pt. Sur to Pigeon Pt. Table 2 summarizes the position of the CU, as described below. The 0.04 spiciness contour was located

about 25 km off Pt. Sur before making a 10 km excursion seaward off Yankee Pt, and returning to a distance of about 10 km off Cypress Pt. Twenty-five km off Santa Cruz, it turned and paralleled the coast increasing the distance to 40 km off Pigeon Pt.

The 26.6 to 26.9 kg/m³ density anomaly layer, which extends from 225 to 500 m, showed the strongest signature, and hence the core, of the CU in terms of spiciness anomaly (Figure 18a). From the horizontal chart, the 0.04 anomaly contour ran north 60 km off Pt. Sur, crossed the canyon and reached a minimum distance of 40 km from the shore off Ano Nuevo before slowly increasing this distance to over 60 km southwest of Pigeon Pt. From the vertical sections, the core of the CU, determined by estimating the center of the positive anomaly area (Figure 5e), was located 60 km offshore of Pt. Sur (or 25 km off the continental slope) at a depth of 300 m, with the area of 0.04 anomaly extending 75 km offshore. Here the width of the CU (the distance from the continental slope to the 0.04 spiciness anomaly contour) was about 50 km. The thickness, determined by measuring the vertical extent of the 0.04 spiciness anomaly area at the core, was 180 m.

Twenty kilometers off Kasler Pt. it turned to the north and paralleled the coast. The core of the CU at this point was 20 km off the slope, 375 m deep, 28 km wide and 420 m thick (Figure 10a). At Yankee Pt. (Figure 11a) the CU core was 10 km off the continental slope, 280 m deep, 37 km wide and 490 thick (Figure 11a). At Cypress Pt., where the CU was closest to Monterey Bay and farthest up the canyon, the core was less than 10 km off the slope and 300 m deep. The width was determined to be 11 km from the distance where the vertical extent of the anomaly layer reaches a minimum in the section shown in Figure 12a, with a

thickness of 390 m near Cypress Pt. The CU waters extended northward across the mouth of Monterey Bay (Figures 1 and 16a). Low values of spiciness anomaly at the most inshore station (station 30) over the 200 m isobath indicate that the CU did not penetrate completely up the canyon.

At Santa Cruz, the core of the CU was only 5 km off the continental slope at a depth of 300 m (Figure 12a). Here the CU was 13 km wide and 410 m thick. Between Santa Cruz and Ano Nuevo (Figure 11a), the core was located 10 km from the continental slope at a depth of 380 m, with a width of about 23 km and a thickness of 290 m. At Ano Nuevo the core was 5 km off the continental slope at a depth of 310 m. The 0.04 anomaly area extended 35 km off the continental slope and was 110 m thick over the fan feature (Figure 1). South of Pigeon Pt. (Figure 13a) the spiciness anomaly appeared to thicken, with a thickness of 320 m, width of 25 km, and centered at a depth of approximately 350 m, 12 km from the slope. Finally, southwest of Pigeon Pt. (Figure 14a), the core of the CU was centered 16 km off the slope at a depth of 320 m, was 31 km wide and 380 m thick.

Between the 26.9 and 27.1 kg/m³ isopycnals (500 to 700 m) (Figure 19a) the spiciness anomaly was less than the layer above. This is an indication that some high spiciness water (>0.08) from the CU was present at this depth. West of Carmel Bay, an area of 0.04 anomaly extended 20 to 30 km to the west over the axis of Monterey Canyon. Directly north of this feature, low spiciness water intrudes towards Cypress Pt. from offshore.

In summary (Table 2), the CU can be traced as a continuous band of spiciness anomaly which was observed adjacent to the continental slope at an average depth of about 300 m in the region off Monterey. The current varies from about 10 to 50 km in width, and between 280 and 375 m in depth. The maximum

TABLE 2. SUMMARY OF PATH OF CU: Location of CU offshore from several coastal locations. Values are given for spiciness anomaly, width, offslope distance of core, depth of core and thickness of core.

Location	Spiciness anomaly	Width (km)	Core (km)	Depth (m)	Thickness (m)
Pt. Sur	>0.04	48	25	300	180
Kasler Pt.	>0.08	28	20	375	420
Yankee Pt.	>0.12	37	10	280	490
Cypress Pt.	>0.12	11	10	300	390
Santa Cruz	>0.12	13	5	300	410
Santa Cruz west	>0.12	23	10	380	290
Ano Nuevo	>0.08	35	5	310	110
Pigeon Pt. south	>0.08	25	12	350	320
Pigeon Pt. west	>0.08	31	16	320	380

spiciness anomaly varies from >0.04 to >0.12 and its distance off the slope varies from 5 to 25 km.

3. Isopycnals

The 26.7 kg/m^3 isopycnal depth (Figure 19b) varied from 260 to 300 m in the region between the 0.04 and 0.08 spiciness anomaly contours previously noted (Figure 18a). Although 40 m shallower than the maximum spiciness anomaly, this isopycnal surface was representative of the core of the CU as determined by spiciness anomaly. The isopycnal depths increase, or slope downwards towards the shore and hence indicate poleward flow along the continental slope from Pt. Sur to Monterey Bay. The 26.7 kg/m^3 surface reaches a depth greater than 310 m in the center of the anticyclonic feature west of Yankee Pt. and shoals to less than 240 m in a cyclonic feature off Ano Nuevo (Figure 20c). The largest depth gradient was seen off Pt. Sur and Kasler Pt. near the anticyclonic feature, indicating the largest horizontal pressure gradient, and hence strongest geostrophic flow.

The 27.0 kg/m³ isopycnal surface (Figure 19b) does show a continuity of isoheights from Pt. Sur to Pigeon Pt. and showed the surface sloping downward towards the coast. A minimum depth of less than 490 m was seen 40 km southwest of Ano Nuevo, which correlates with the low spiciness CC water intruding towards Cypress Pt. between the 26.9 and 27.1 kg/m³ layer (Figure 19a). The strongest gradient of the 27.0 kg/m³ isopycnal surface follows the offshore side of the high spiciness anomaly at the 26.6 to 26.9 kg/m³ layer (Figure 18a).

4. Dynamic heights

The dynamic heights at 200 db referenced to 500 dbar (Figure 20c) reveal a poleward, offshore geostrophic flow (the CU) off Pt. Sur. The CU was part of an anticyclonic circulation which extended almost 40 km seaward. The gradients in dynamic height were the greatest off Kasler Pt., indicating the strongest flow approximately 40 to 45 km offshore ($V \sim 25$ to 30 cm/s). North of Yankee Pt. the gradient between isosteres decreased ($V \sim 15$ cm/s) as the flow moves closer to shore (25 km off Cypress Pt). At Cypress Pt. the flow turned cyclonically to parallel the mouth of Monterey Bay and cross the canyon. The gradient of isosteres decreased as the CU approaches Santa Cruz indicating a weakening of the flow ($V \sim 5$ cm/s). West of Santa Cruz, the 0.39 m²/s² isostere paralleled the shore, then turned shoreward after passing the fan feature, suggesting that a dynamic trough extended to the shore in this region. Southwest of Pigeon Pt., the poleward (westward) flow resumed, passing between a large cyclonic eddy centered 50 km offshore on the south side, and the continental slope to the north. A relaxation in the gradient of dynamic heights indicated weak flow (<5 cm/s) to the west of this region. The dynamic height contours were continuous from Pt. Sur to Pigeon Pt. like the 26.6

to 26.9 kg/m^3 spiciness anomaly (Figure 18a), with the pattern of the poleward flow from Pt. Sur to Pigeon Pt. interrupted only at Ano Nuevo.

5. Effect of bathymetry

At Pt. Sur the westward component of flow was apparently caused by a deflection of the CU by the broadened continental margin (Figure 1). Near Kasler Pt. the width of the upper continental margin narrows where the flow entered the canyon. At Yankee Pt. the width of the upper margin narrows further where the CU flowed over one of the steeper sections of the south wall of the Monterey Canyon. The CU off Cypress Pt. was paralleled the steepest part of the canyon wall. As the CU turned toward Santa Cruz, it traversed directly over the center of the Monterey Canyon and collided with the eastern slope of the fan. The flow followed the edge of the fan to the west and moved onshore into Ascension Canyon off Ano Nuevo. At Ano Nuevo the width of the upper margin (Figure 1) is relatively narrow, though the top of the continental shelf, at a depth of 200 m, extends over 10 km seaward. Beyond Ano Nuevo, the widening of the upper margin apparently weakened the flow and forced it farther offshore as it continued past Pigeon Pt.

A comparison of the spiciness anomalies over the 26.6 and 26.9 kg/m^3 density anomaly surfaces, the depth of the 26.7 kg/m^3 isopycnal, and 200/500 dbar dynamic heights to the position of the upper margin (Figures 23a, 23b, and 23c) reveals that the flow did not appear to follow any particular isobath. However, the distance that the 0.04 anomaly extended from the continental slope was proportional to the width of the upper margin. Widths of the upper margin (200 to 1000 m) and CU as indicated by spiciness anomaly are shown in Table 3 and Figure 24. While Figure 24 does not show a strong correlation between CU and upper

margin widths, it does suggest that a wider margin does force a widening of the CU. Off Pt. Sur, the 0.08 spiciness anomaly contour (Figure 18a) has a shape similar to the 200 isobath. However, these contours were out of phase with the spiciness anomaly contour lagging the bathymetry suggesting that the offshore deflection persists downstream.

B. NEAR-SURFACE PATTERNS

In vertical sections, patterns of salinity, temperature, density anomaly and spiciness above and below 200 m differed due to the dominance of upwelling in near-surface waters.

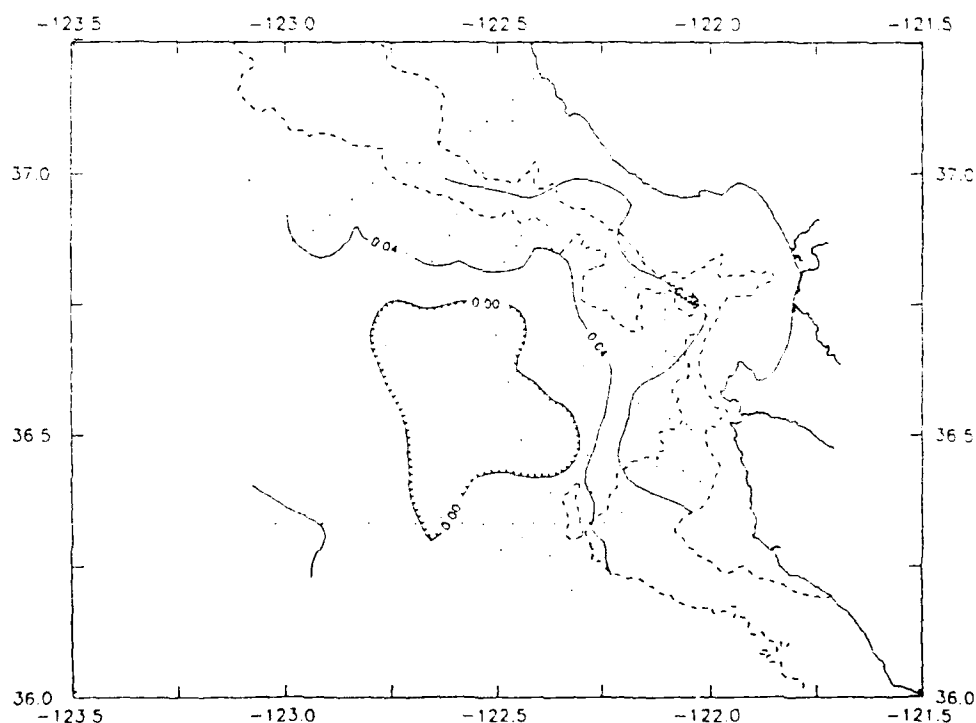


Figure 23a. Spiciness anomaly averaged over 26.6 to 26.9 kg/m³ density anomaly layer with upper margin overlaid: A close correlation between the flow pattern from spiciness anomalies and the position of the upper margin was not observed. The width of the CU does seem to be proportional to the width of the upper margin.

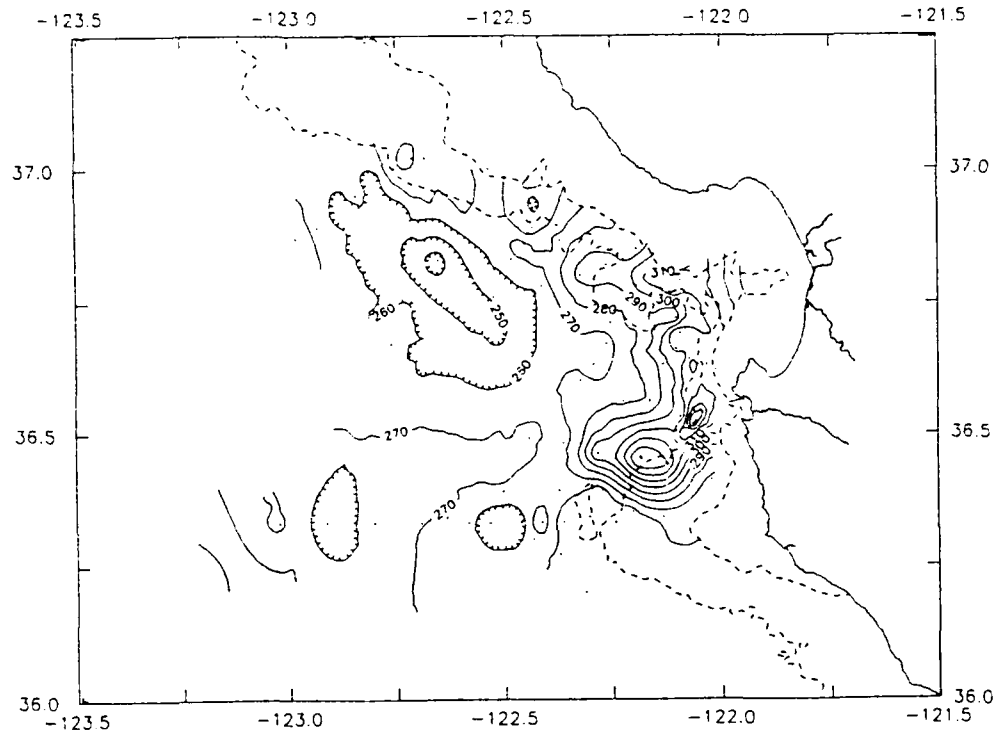


Figure 23b. Depth of the 26.7 kg/m^3 isopycnal with upper margin overlaid: Little correlation was observed between the depth of the 26.7 kg/m^3 isopycnal and position of the upper margin.

The chart of dynamic heights at the surface referenced to 200 dbar (Figure 20a) showed a reversal of horizontal flow from the 200/500 dbar layer (Figure 20c). In contrast to the lower layer, where the high was at the coast and the low offshore, the near-surface high was offshore and the low was at the coast. If 200 dbar were a level of no motion, this would require southward flow from Yankee Pt. past Pt. Sur, an area of anticyclonic circulation about 50 km west of Yankee Pt., and a trough about 50 km southwest of Pigeon Pt. associated with onshore flow. Satellite imagery for 24 May (Figure 22) also indicates an anticyclonic flow.

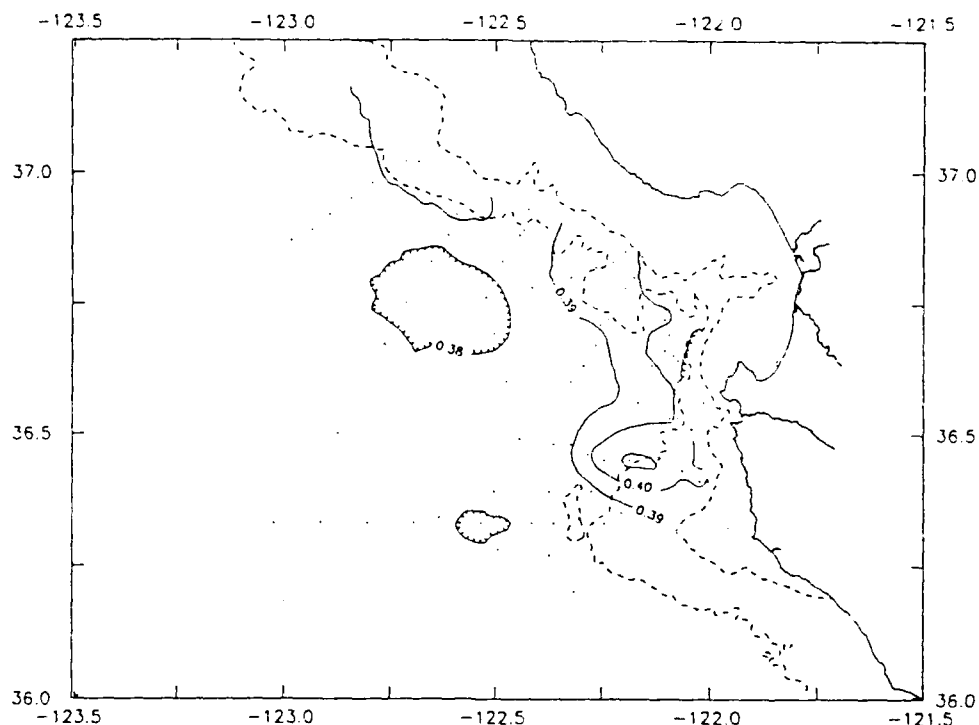


Figure 23c. Dynamic heights at 200/500 dbar with upper margin overlaid: A rough correlation was observed between the 200/500 dbar dynamic heights and position of the upper margin. The flow did follow the coastline with the largest gradients over the upper margin.

Table 3. WIDTHS OF CU AND UPPER MARGIN

Location	CU (km)	Upper Margin (km)
Pt. Sur	48.5	18.5
Kasler Pt.	28.0	17.8
Yankee Pt.	37.0	6.8
Cypress Pt.	11.0	4.2
Santa Cruz (south)	13.5	3.0
Santa Cruz (southwest)	23.0	12.8
Ano Nuevo	35.0	12.0
Pigeon Pt. (south)	25.0	8.1
Pigeon Pt. (west)	31.0	12.3

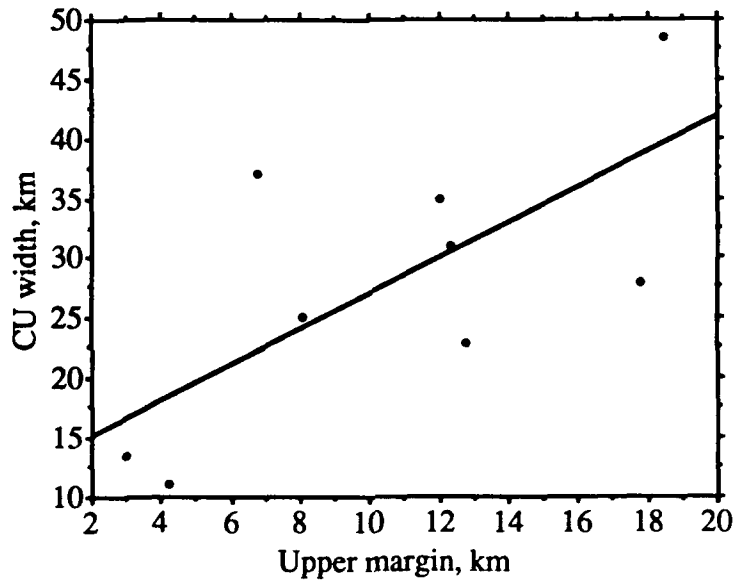


Figure 24. Width of CU versus width of upper margin: The widths of the CU and upper margin are weakly correlated.

In the upper 50 m of the water column, between the 25.6 and 26.0 density anomaly surfaces (Figure 15a), high positive spiciness anomalies were found only in small areas paralleling the coast between Pt. Sur and Santa Cruz, and in a larger area centered approximately 40 km off Pigeon Pt. There was no correlation with bathymetry at this level.

Between the 26.0 and 26.4 kg/m³ density anomalies (Figure 16a), the 0.04 spiciness anomaly contour paralleled the coast from Pt. Sur to Santa Cruz making a 20 km excursion offshore west of Yankee Pt. Extending from 50 to 150 m, this layer was also not correlated with the isobaths.

No correlation was found between surface and subsurface flows. The surface circulation (Figure 20a) consisted of cyclonic and anticyclonic features and showed no continuous isoheights. While the subsurface flow (Figure 20c) also had areas of implied cyclonic and anticyclonic circulation, only the area off Yankee Pt. showed any correlation with the surface flow.

V. CONCLUSIONS AND RECOMMENDATIONS

From a hydrographic survey in May 1989, the California Undercurrent, as characterized by waters exhibiting high spiciness, was found to flow poleward along the continental shelf at a depth of about 300 m off Monterey. It was deflected offshore at Pt. Sur by the continental shelf, then crossed the Monterey Canyon, and turned cyclonically following the continental slope to the northwest past Santa Cruz and Pigeon Pt.

Although the use of the state variable spiciness proves to be very useful for tracing water masses, it did not necessarily correlate with the observed velocity field off Pt. Sur. Lagrangian techniques may yield a better congruence of properties; the pattern of spiciness anomaly should be predicted by the Green's function of the float trajectories (Davis 1983). The kinematics of the velocity field were best measured with Pegasus or current meters. However, the water mass analysis applied here is an effective and economical method of describing the general circulation of this region, and clearly defines the extent of the CU off Monterey.

Though not specifically addressed in this thesis, there are tactical applications to this study. The northward transport of the CU causes a shoaling of the SOFAR channel, about 100 km offshore. Off Monterey, the axis of the SOFAR channel can be within 500 m of the surface, allowing easier access by listening equipment utilized by surface ships.

Recommendations for future studies would include Lagrangian float studies and detailed hydrographic surveys to follow the path of the CU to the north and south.

REFERENCES

- Chelton, D. B., 1984, Seasonal variability of alongshore geostrophic velocity off central California, *J. Geophys. Res.*, *89*, 3473-3486.
- Chelton, D. B., A. W. Bratkovich, R. L. Bernstein, and P. M. Kosro, 1988, Poleward flow off central California during the spring and summer of 1981 and 1984, *J. Geophys. Res.*, *93*, 10,604-10,620.
- Davis, R. E., 1983, Oceanic property transport, Lagrangian particle statistics, and their prediction, *J. Mar. Res.*, *41*, 163-194.
- Flament, P., submitted 1989, A note on seawater spiciness and diffusive stability, *Deep Sea Res.*
- Hickey, B. M., 1979, The California Current system-hypothesis and facts, *Prog. Oceanogr.*, *8*, 191-279.
- Lynn, R. J., and J. J. Simpson, submitted 1989, The influence of bathymetry upon the flow of the undercurrent off Southern California, *J. Geophys. Res.*
- Reid, R. L. and R. A. Schwartzlose, 1962, Direct measurements of the Davidson Current off central California, *J. Geophys. Res.*, *67*, 2491-2497.
- Spain, P. F., D. L. Dorson, and H. T. Rossby, 1981, Pegasus: A simple, acoustically tracked, velocity profiler, *Deep Sea Res.*, *28A*, 1553-1567.
- Sverdrup, H. U., R. H. Johnson, M. W. Fleming, 1942, *The Oceans*, Prentice-Hall, Inc. Englewood Cliffs, NJ, 1066 pp.
- UNESCO, 1987, International Oceanographic Tables, Vol. 4. *Unesco Tech. Paper in Mar. Sci.*, *40*, 101.
- Wickham, J. B., A. A. Bird, and C. N. K. Mooers, 1987, Mean and variable flow over the central California continental margin, 1978-1980, *Cont. Shelf Res.*, *7*, 827-849.

APPENDIX A

CTD DATA CALIBRATION

175 water samples were collected during the CTD casts for use in calibration of conductivity measured by the Neil-Brown CTD. Standard practice would be to complete a regression of sample salinity versus CTD salinity and then apply this regression to the entire data set for calibration. However the resultant regression showed considerable variability. Plotting bottle salinity minus CTD salinity versus pressure revealed a distinct pressure dependence of salinity for the CTD used during the cruise. This resulted in larger differences between sample salinity and CTD salinity for the deeper samples (fig A1).

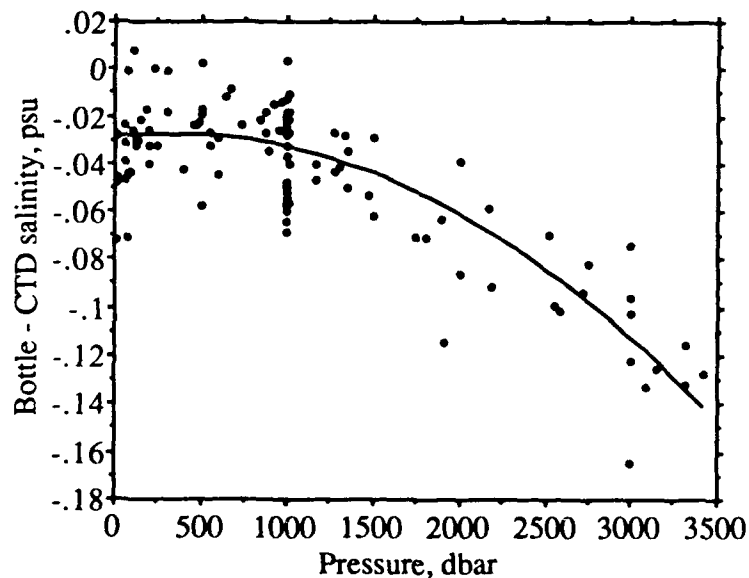


Figure A1. Pressure dependence of CTD salinities: Difference between sample salinities and CTD salinities as a function of pressure. Solid line is parabolic least squares fit to calibration data points.

A parabolic pressure correction was determined that gave salinity difference

(bottle salinity minus CTD salinity) as a function of pressure, $Y = -0.029 + (7.939E-6)X - (1.193E-8)X^2$. This was then added back to the CTD salinity thereby effectively removing the pressure dependence (fig A2). This produced a simple polynomial fit, $Y = -0.27 + (1.062)X - (0.032)X^2$, between bottle salinity and CTD salinity (fig A3) which was then applied to the entire data set as a calibration constant.

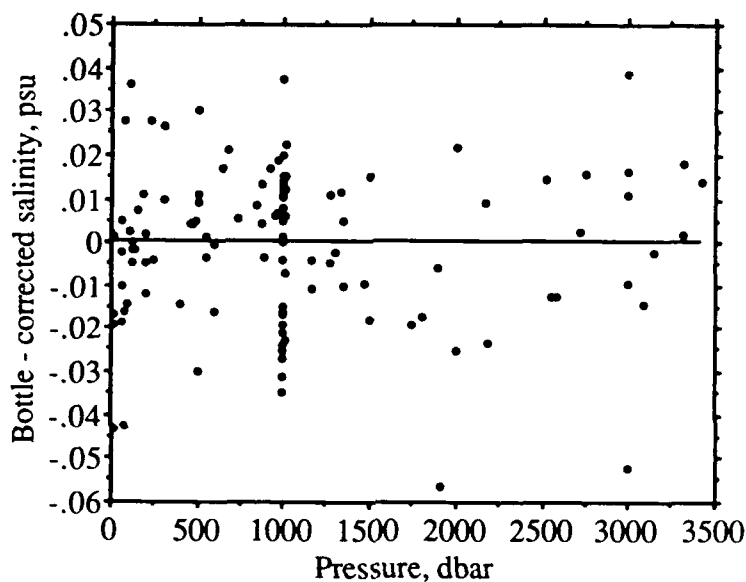


Figure A2. Pressure effect removed: difference between bottle salinity and CTD salinity after removal of pressure dependence.

However, removal of the pressure dependence also removed the observed deep salinity gradient. This was corrected in a final step as follows:

$$\text{deep salinity correction} = \text{salinity} \times 0.00002 \times (\text{pressure} - 3000 \text{ db})$$

for pressures greater than 3000 db.

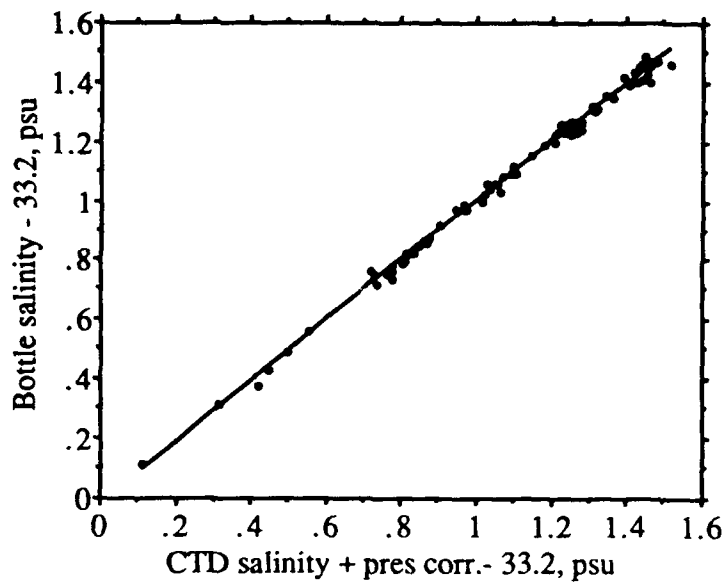


Figure A3. Final regression: Bottle salinity minus 33.2 versus CTD salinity + pressure correction - 33.2. Final calibration applied to salinity.

INITIAL DISTRIBUTION LIST

	No. Copies
1. Defense Technical Information Center Cameron Station Alexandria, VA 22304-6145	2
2. Library, Code 0142 Naval Postgraduate School Monterey, CA 93943-5100	2
3. Chairman (Code OC/Co) Department of Oceanography Naval Postgraduate School Monterey, CA 93943-5000	1
4. Chairman (Code ME/Re) Department of Meteorology Naval Postgraduate School Monterey, CA 93943-5000	1
5. Professor Curtis A. Collins (Code OC/Co) Department of Oceanography Naval Postgraduate School Monterey, CA 93943-5000	1
6. Professor Frank Schwing Pacific Fisheries Environmental Group P. O. Box 831 Monterey, CA 93942	1
7. LT Alan J. Robson USS TARAWA (LHA-1) FPO San Francisco, CA 96622-1600	1
8. Director Naval Oceanography Division Naval Observatory 34th and Massachusetts Avenue NW Washington, DC 20390	1

- | | | |
|-----|---|---|
| 9. | Commander
Naval Oceanography Command
Stennis Space Center
Bay St. Louis, MS 39529-5000 | 1 |
| 10. | Commanding Officer
Naval Oceanographic Office
Stennis Space Center
Bay St. Louis, MS 39522-5001 | 1 |
| 11. | Commanding Officer
Fleet Numerical Oceanography Center
Monterey, CA 93940-5005 | 1 |
| 12. | Commanding Officer
Naval Ocean Research and Development Activity
Stennis Space Center
Bay St. Louis, MS 39522-5004 | 1 |
| 13. | Director
Naval Oceanographic and Atmospheric
Research Laboratory (West)
Monterey, CA 93943-5006 | 1 |
| 14. | Chairman, Oceanography Department
U. S. Naval Academy
Annapolis, MD 21402 | 1 |
| 15. | Chief of Naval Research
800 N. Quincy Street
Arlington, VA 22217 | 1 |
| 16. | Office of Naval Research (Code 420)
Naval Ocean Research and Development Activity
800 N. Quincy Street
Arlington, VA 22217 | 1 |
| 17. | Scientific Liason Office
Office of Naval Research
Scripps Institution of Oceanography
La Jolla, CA 92037 | 1 |

- | | |
|--|---|
| 18. Library
Scripps Institution of Oceanography
P.O. Box 2367
La Jolla, CA 92037 | 1 |
| 19. Library
Department of Oceanography
University of Washington
Seattle, WA 98105 | 1 |
| 20. Library
CICESE
P.O. Box 4803
San Ysidro, CA 92073 | 1 |
| 21. Library
School of Oceanography
Oregon State University
Corvallis, OR 97331 | 1 |
| 22. Commander
Oceanographic Systems Pacific
Box 1390
Pearl Harbor, HI 96860 | 1 |
| 23. Nan Bray
Center For Coastal Studies
La Jolla, CA 92093 | 1 |
| 24. Ronald J. Lynn
Southwest Fisheries Center
National Marine Fisheries Service
National Oceanic and Atmospheric Administration
La Jolla, CA 92093 | 1 |
| 25. James J. Simpson
Scripps Institution of Oceanography
La Jolla, CA 92037 | 1 |
| 26. Newell Garfield (Code OC/Gf)
Department of Oceanography
Naval Postgraduate School
Monterey, CA 93943-5000 | 1 |

- | | |
|---|---|
| 27. Dr. Nicholas Fofonoff
Department of Physical Oceanography
Woods Hole Oceanographic Institution
Woods Hole, MA 02543 | 1 |
| 28. Dr. Francisco Chavez
Monterey Bay Aquarium Research Institute
P. O. Box 160
Central Avenue
Pacific Grove, CA 93950-0020 | 1 |
| 29. Dr. Louis Codispoti
Monterey Bay Aquarium Research Institute
P. O. Box 160
Central Avenue
Pacific Grove, CA 93950-0020 | 1 |
| 30. Dr. Bill Broenkow
Moss Landing Marine Laboratory
P. O. Box 223
Moss Landing, CA 95039 | 1 |
| 31. Dr. Adriana Huyer
College of Oceanography
Oregon State University
Corvallis, OR 97331 | 1 |
| 32. Prof. Joseph Reid
Scripps Institution of Oceanography
La Jolla, CA 92037 | 1 |
| 33. Lt. Tim Tisch
Naval Postgraduate School
SMC 2758
Monterey, CA 93943-5000 | 1 |